JPET Fast Forward. Published on June 5, 2018 as DOI: 10.1124/jpet.118.248278
This article has not been copyedited and formatted. The final version may differ from this version.

JPET#248278

NOVEL POLYPHENOLS THAT INHIBIT COLON CANCER CELL GROWTH AFFECTING CANCER CELL METABOLISM

Marta Gómez de Cedrón, Teodoro Vargas, Andrés Madrona, Aranza Jiménez, María-Jesús Pérez-Pérez, José-Carlos Quintela, Guillermo Reglero, Ana San-Félix, Ana Ramírez de Molina

Molecular Oncology and Nutritional Genomics of Cancer, IMDEA-Food Institute, CEI UAM+CSIC, Madrid 28049, Spain (M.G.d.C., T.V., G.R., A.R.d.M.); Instituto de Química Médica (IQM-CSIC), Juan de la Cierva 3, Madrid 28006, Spain (A.M., A.J., M.J.P.-P., A. S.-F.); Natac Biotech S.L., Parque Científico de Madrid, Campus de Cantoblanco, Madrid 28049, Spain (J.-C.Q); Actual address: Novartis Farmacéutica S.A. Gran Vía de les Corts Catalanes, 764, Barcelona, 08013, Spain (A.M.); Actual address: Agencia Española de Medicamentos y productos Sanitarios, Campezo 1, Edificio 8, Madrid 28022 (A.J.)

Downloaded from jpet.aspetjournals.org at ASPET Journals on April 19, 2024

JPET Fast Forward. Published on June 5, 2018 as DOI: 10.1124/jpet.118.248278
This article has not been copyedited and formatted. The final version may differ from this version.

Running Title

Polyphenols targeting cancer cell metabolism

Corresponding author: Ana Ramírez de Molina. IMDEA Food Institute, Crta. Cantoblanco 8, 28049, Madrid, Spain. Tel.: +34 912796957; fax: +34 911880756.

E-mail address: ana.ramirez@imdea.org

Corresponding author: Ana San-Félix. Instituto de Química Médica (IQM-CSIC), Juan de la Cierva 3, 28006, Madrid, Spain. Tel.; +34 912587617; +34 915644853

E-mail address: anarosa@iqm.csic.es

Number of text pages: 36

Number of tables: 2

Number of figures: 9

Number of references: 58

Number of words in the *Abstract:* 178

Number of words in the *Introduction:* 682

Number of words in the *Discussion:* 641

Abbreviations: DIPEA, *N,N*-diisopropylethylamine; DMAP, dimethylaminopyridine; ECAR, extra-cellular acidification rate; FCCP, cyanide-4-(trifluoromethoxy)phenylhydrazone; HATU, (1-[bis(dimethylamino)methylene]-1H-1,2,3-triazolo[4,5-b]pyridinium 3-oxid hexafluorophosphate); MOM, methoxymethyl; OCR, oxygen consumption rate; TEA, trimethylamine; TFH; tetrahydrofurane

Recommended section assignment: Drug Discovery and Traslational Medicine

Address correspondence to: Ana Ramírez de Molina. IMDEA Food Institute, Crta. Cantoblanco 8, 28049, Madrid, Spain. Tel.: +34 912796957; fax: +34 911880756.

E-mail address: ana.ramirez@imdea.org

Downloaded from jpet.aspetjournals.org at ASPET Journals on April 19, 2024

JPET Fast Forward. Published on June 5, 2018 as DOI: 10.1124/jpet.118.248278
This article has not been copyedited and formatted. The final version may differ from this version.

Abstract

New series of polyphenols with a hydrophilic galloyl based "head" and a hydrophobic *N*-acyl "tail", linked through a serinol moiety, have been synthesized and tested against colon cancer cell growth. Our structure activity relationship studies revealed that galloyl moieties are essential for growth inhibition. Moreover, the length of the *N*-acyl chain is crucial for the activity. Introduction of a (*Z*) double bond in the acyl chain increased the anti-cancer properties. Our findings demonstrate that **16**, the most potent compound within this series, has inhibitory effects on colon cancer cell growth and metabolism (glycolysis and mitochondrial respiration) at the same time that activates AMPK and induces apoptotic cell death. Based on these results we propose that **16** might reprogram colon cancer cell metabolism through AMPK activation. This might lead to alterations on cancer cell bioenergy compromising cancer cell viability. Importantly, these anti-proliferative and pro-apoptotic effects are selective for cancer cells. Accordingly, these results indicate that **16**, with an unsaturated C18 chain, might be a useful prototype for the development of novel colon cancer cell growth inhibitors affecting cell metabolism.

Visual Abstract

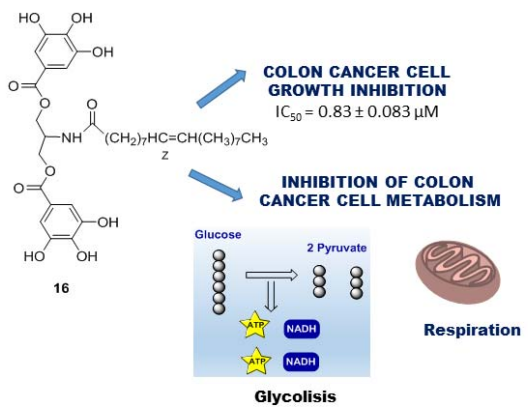

Downloaded from jpet.aspetjournals.org at ASPET Journals on April 19, 2024

JPET Fast Forward. Published on June 5, 2018 as DOI: 10.1124/jpet.118.248278
This article has not been copyedited and formatted. The final version may differ from this version.

1. Introduction

In recent years, the understanding of differences in cell metabolism between normal and cancer cells has been considered essential in the design and development of new anticancer drugs. In this respect, proliferating cancer cells exhibit a higher dependency on aerobic glycolysis than normal cells (Lopez-Lazaro, 2010; Marchetti et al., 2014), a phenomenon known as the "Warburg effect" (Warburg, 1956). This metabolic difference has led to the hypothesis that inhibition of glycolysis may preferentially kill cancer cells and may have significant therapeutic implications (Pelicano et al., 2006). Indeed, several glycolytic inhibitors (2-deoxy-D-glucose, lonidamine, 3-bromopyruvate and dichloroacetate) have shown anticancer activities both *in vitro* and *in vivo*, and some of them have entered clinical trials. However, they show important drawbacks (low potency, instability…) that may limit their use as therapeutic drugs. Thus, development of new generations of glycolytic inhibitors with high potency, chemical stability and good safety profiles represents an important task in the anti-cancer field.

In addition, cancer cells and normal cells metabolize oxygen (O_2) differently. Normal cells use oxygen (O_2) to generate energy in the form of ATP at mitochondria, meanwhile cancer cells use O_2 to generate high levels of reactive oxygen species (ROS), and aerobic glycolysis is used to provide energy and satisfy structural demands. This difference in the metabolism of O_2 can be also exploited to kill cancer cells selectively (Marchetti et al., 2014).

Lately, natural and synthetic polyphenols have become a focus of interest on cancer chemoprevention and chemotherapy. In fact, epidemiological studies suggest that the intake of polyphenols may protect against tumor growth (Arts and Hollman, 2005; Neuhouser, 2004), particularly gastrointestinal cancers (Pierini et al. 2008). The growth inhibition induced by polyphenols in tumor cells include several inhibitory mechanisms such as the activation of caspases, cell cycle arrest and the inhibition of survival or proliferative signaling pathways (NF-kB, JAK/STAT) among others (Gonzalez-Vallinas et al., 2013; Hadi et al., 2007; Kubatka et al., 2016; Zhang et al., 2015).

Moreover, there are many examples of dietary polyphenols affecting different metabolic pathways of cancer cells (Cerella et al., 2013). Flavonoids, quercetin, oleuropein, hydroxytyrosol and epigallocatechin-3-gallate (ECGC) have been shown to affect glycolysis-related factors, meanwhile others like curcumin, or resveratrol target mitochondrial metabolism inducing cell death and/or apoptosis in a variety of cancer models (Boyer et al., 2012; Kim et al., 2009; Teiten et al., 2010). In many cases, the underlying mechanism is associated to 5'AMP-activated kinase (AMPK) activation (Hung, et al., 2012; Shin et al., 2009).

Downloaded from jpet.aspetjournals.org at ASPET Journals on April 19, 2024

JPET Fast Forward. Published on June 5, 2018 as DOI: 10.1124/jpet.118.248278
This article has not been copyedited and formatted. The final version may differ from this version.

AMPK is a central metabolic sensor that regulates anabolism or catabolism in response to energetic demands and/or oxidative stress. When activated, AMPK inhibits the main anabolic pathways that promote cell growth (DG., 2014; Li et al., 2015; Hardie, 2014). In cancer, where the energetic demands are elevated to support rapid cell growth and division, AMPK activators can be suitable candidates for therapeutic intervention. In fact, AMPK is emerging as a promising target for cancer prevention and therapy (Luo et al., 2010).

As a part of an ongoing work in our laboratories directed to the synthesis and biological evaluation of polyphenols as antiviral and antibacterial agents (Flores et al., 2014; Rivero-Buceta et al., 2015a; Rivero-Buceta et al., 2015b), we prepared molecules of general formula **I**, with a hydrophilic "head", composed of two galloyl (3,4,5-trihydroxybenzoyl) units (R^1), and a hydrophobic "tail" (R) composed of an *N*-acyl-chain, linked through a serinol moiety (Figure 1). Systematic modifications have been performed in these compounds. First, the effect of the *N*-acyl chain length of the hydrophobic tail was analyzed by introduction of different aliphatic acyl residues with variable number of carbons (C2, C7, C11 and C17). The effect of unsaturation (one or two double bonds) on the hydrophobic "tail" was also analyzed. Modifications on the "head" were also performed by replacing the galloyl moieties, with 3 OHs, by other phenolic units with 2 OHs. Finally, ethanolamine, instead of serinol, was used as a linker.

For all these compounds inhibition of colon cancer cell proliferation and colon cancer energetic metabolism (glycolysis and oxygen consumption), together with activation of AMPK and induction of apoptotic cell death have been determined and are herein described.

Downloaded from jpet.aspetjournals.org at ASPET Journals on April 19, 2024

JPET Fast Forward. Published on June 5, 2018 as DOI: 10.1124/jpet.118.248278
This article has not been copyedited and formatted. The final version may differ from this version.

2. Materials and Methods

2.1. Synthesis

2.1.1. General Methods

Commercial reagents and solvents were used as received from the suppliers without further purification unless otherwise stated. Dichloromethane was dried prior to use by distillation from CaH_2 and stored over Linde type activated 4Å molecular sieves.

Analytical thin-layer chromatography (TLC) was performed on aluminum plates pre-coated with silica gel 60 (F_{254}, 0.25 mm). Products were visualized using an ultraviolet lamp (254 and 365 nm) or by heating on a hot plate (approx. 200 ºC), directly or after treatment with a 5% solution of phosphomolybdic acid or vanillin in ethanol.

The compounds were purified by: a) flash column chromatography on silica gel (60 Merck 230-400 mesh), b) trituration with cold diethyl ether and dichloromethane.

NMR spectra (^{1}H, ^{13}C NMR) were recorded on a Varian UNIT INOVA-300 (300 MHz), Bruker AVANCE 300 (300 and 75 MHz), Varian INOVA-400 (400 and 100 MHz), Varian MERCURY-400 (400 and 100 MHz) and Varian-500 (500 and 125 MHz) spectrometers, using $(CD_3)_2SO$ and $CDCl_3$ as solvents. Chemical shift (δ) values are reported in parts per million (ppm) relative to tetramethylsilane (TMS) in 1H and $CDCl_3$ ($\delta = 77.0$) in ^{13}C NMR. Coupling constant (J values) are reported in hertz (Hz) and multiplicities of signals are indicated by the following symbol: s (singlet), d (doublet), t (triplet), q (quadruplet), m (multiplet) and bs (broad singlet). Some two-dimensional spectra (COSY, HSQC and HMBC) were performed to identify the structure.

Final compounds were lyophilized using a Telstar 6-80 system.

*2.1.2. General procedure for the synthesis of serinol derivates **2-6***

A stirred solution of 2-amino-1,3-propanediol (serinol) **1** (1 eq) and triethylamine (TEA) in MeOH (10 mL) was cooled at -20 ºC and treated drowpwise with a solution of the corresponding acyl chloride (1.1 eq) in THF (5 mL). The reaction mixture was allowed to warm to room temperature and stirred overnight. Then it was poored into brine and extracted with dichloromethane (3 x 10 mL). The combined organic phases were washed with brine, dried over $MgSO_4$ and concentrated under reduced pressure. The residue was

Downloaded from jpet.aspetjournals.org at ASPET Journals on April 19, 2024

JPET Fast Forward. Published on June 5, 2018 as DOI: 10.1124/jpet.118.248278
This article has not been copyedited and formatted. The final version may differ from this version.

purified by flash column chromatography on silica gel using as eluent EtOAc/MeOH (10:1 to 7:1) to provide the corresponding *N*-acyl serinol derivatives.

2.1.3. N-propanoylserinol ***(2)***

According to the general procedure serinol (150 mg, 1.64 mmol) was treated with propanoyl chloride (1.86 mmol, 0.16 mL) and triethylamine (0.4 mL) to give the title compound (202 mg, 81%) as an amorphous white solid. ^{1}H NMR (400 MHz, DMSO-d_6) δ 7.40 (d, J = 8.1 Hz, 1H, NH), 4.55 (t, J = 5.5 Hz, 2H, OH), 3.74-3.64 (m, 1H, CH), 3.37 (t, J = 5.6 Hz, 4H, CH_2OH), 2.06 (t, J = 7.4 Hz, 2H, $CH_2C{=}O$), 1.51 – 1.42 (m, 2H, CH_2), 1.30-1.15 (m, 8H, CH_2), 0.86 (t, J = 6.8 Hz, 3H, CH_3).

*2.1.4. N-dodecanoyl serinol (**3**)*

According to the general procedure serinol (200 mg, 2.19 mmol) was treated with dodecanoyl chloride (625 mg, 2.85 mmol) and triethylamine (0.6 mL) to give the title compound (478 mg, 80 %) as an amorphous white solid. Characterization of this compound is consistent with those found in the literature (Boyer et al., 2012; Kim et al., 2009).

*2.1.5. N-octadecanoyl serinol (**4**)*

According to the general procedure serinol (150 mg, 1.64 mmol) was treated with octadecanoyl chloride (545.24 mg, 1.80 mmol) and triethylamine (0.4 mL) to give the title compound (421 mg, 75%) as an amorphous white solid. Characterization of this compound is consistent with those found in the literature (Bieberich et al., 2002a; Merg et al., 2015; Shulz and Robins, 2004).

*2.1.6. (N-oleoyl serinol) (**5**)*

Serinol (55 mg, 0.60 mmol) was treated with 9-octadecenoyl chloride (oleoyl chloride) (198.6 mg, 0.66 mmol,) and triethylamine (0.1 mL) to give the title compound (149 mg, 70%) as an amorphous white solid. Characterization of this compound is consistent with those found in the literature (Bieberich et al., 2002a; Landau and Siegel, 2014; Osornio et al., 2012).

*2.1.7. N-linoleoyl serinol (**6**)*

Downloaded from jpet.aspetjournals.org at ASPET Journals on April 19, 2024

JPET Fast Forward. Published on June 5, 2018 as DOI: 10.1124/jpet.118.248278
This article has not been copyedited and formatted. The final version may differ from this version.

Serinol (55 mg, 1.64 mmol) was treated with linoleoyl chloride (1.81 mmol, 0.6 mL) and triethylamine (0.1 mL) to give the title compound (169 mg, 79 %) as an amorphous white solid. Characterization of this compound in the literature was incomplete (Oette and Tschung, 1980). Missing data (NMR) was now included. ^{1}H NMR (400 MHz, DMSO-d_6) δ 7.41 (d, J = 8.1 Hz, 1H, NH), 5.35 – 5.27 (m, 2H, CH=CH), 4.56 (t, J = 5.5 Hz, 2H, OH), 3.74 – 3.63 (m, 1H, CH, NH), 3.38 (t, J = 6.0 Hz, 4H, CH_2OH), 2.05 (t, J = 7.5 Hz, 2H, CH_2C=O), 2.01 – 1.92 (m, 4H, CH_2HC= $CHCH_2$), 1.50 – 1.42 (m, 2H, CH_2), 1.34 – 1.14 (m, 22H, CH_2), 0.85 (t, J = 6.8 Hz, 3H, CH_3).

*2.1.8. 3,4,5-tris(methoxymethoxy)benzoic acid (**7**)*

To a cooled (0 ºC) mixture of methylgallate (500 mg, 2.71 mmol) and DIPEA (1.6 mL, 8.96 mmol) in dichloromethane (20 mL) was added methoxymethyl chloride (MOM-Cl) (0.7 mL, 8.97 mmol). The reaction was stirred at 0 ºC for 20 min and then at room temperature overnight. The solvent was evaporated to dryness and the residue was dissolved in ethyl acetate (20 mL) and washed successively with a saturated solution of ammonium chloride (3 x 20 mL) and water (3 x 20 mL). The organic layer was dried over anhydrous Na_2SO_4, filtered, and concentrated under vacuum. The residue was then purified by flash column chromatography using hexane/EtOAc (6:1 to 2:1) as the eluent to give 543 mg (63 %) of methyl 3,4,5-tris(methoxymethoxy)benzoate as a white amorphous solid that was used for the next step. ^{1}H-RMN (300 MHz, CD_3Cl) δ 7.51 (s, 2H, H-Ph), 5.24 (s, 4H, 2 x CH_2MOM), 5.13 (s, 2H, 1 x CH_2MOM), 3.83 (s, 3H, OCH_3), 3.51 (s, 3H, 1 x CH_3MOM), 3.41 (s, 6H, 2 x CH_3MOM).

To a solution containing the above mentioned methyl ester derivative (540 mg, 1.71 mmol) in THF (15 mL) at 0 ºC (ice-bath), a solution of LiOH·H_2O (220 mg, 5.12 mmol) in water (10 mL) was added, and the mixture was stirred at room temperature overnight. Then 1 N hydrochloric acid aqueous solution was added to reach pH = 2, and volatiles were evaporated to dryness. The residue was dissolved in ethyl acetate (20 mL) and washed with H_2O (3 × 20 ml). The organic phase was dried over anhydrous Na_2SO_4, filtered and evaporated to dryness to give 488.7 mg (95%) of the title compound that was directly used for the next step. Characterization of this compound is consistent with those found in the literature (Gazak et al., 2011).

*2.1.9. General coupling procedure for the synthesis of the MOM protected intermediates **8-12***

A solution of the MOM protected gallic acid **7** (Gazak et al., 2011) (2.2 eq), HATU (2.2 eq) and DMAP (1.25 eq) in dry CH_2Cl_2 (10 ml) was stirred at room temperature for 15 minutes and then added to a second

Downloaded from jpet.aspetjournals.org at ASPET Journals on April 19, 2024

JPET Fast Forward. Published on June 5, 2018 as DOI: 10.1124/jpet.118.248278
This article has not been copyedited and formatted. The final version may differ from this version.

solution, also stirred for 15 min, containing the corresponding serinol derivate (1eq) and DMAP (1.25 eq) in dry CH_2Cl_2 (10 ml). The mixture was stirred at room temperature overnight and then evaporated to dryness. The residue was dissolved in ethyl acetate (20 mL) and washed successively with saturated solutions of citric acid (3 x 20 mL), $NaHCO_3$ (3 x 20 mL) and NaCl (1 x 20 mL). The organic layer was dried over anhydrous Na_2SO_4, filtered, and concentrated under vacuum. The residue was then purified by flash column chromatography using hexane/EtOAc (10:1 to 1:1) as the eluent.

*2.1.10. Bis-O-[3,4,5-tris(methoxymethoxy)galloy]-N-propanoyl serinol (**8**)*

Following the general procedure, **2** (50 mg, 0.34 mmol) was treated with **7** (Gazak et al., 2011) (226.24 mg, 0.74 mmol), HATU (284.4 mg, 0.74 mmol) and DMAP (226.0 mg, 1.84 mmol) to afford 366 mg (75 %) of the title compound as an amorphous white solid. ^{1}H-RMN (300 MHz, CD_3Cl) δ 7.52 (s, 4H, Ph), 6.03 (d, J = 8.30 Hz, 1H, NH), 5.24 (s, 8H, 4 x CH_2MOM), 5.22 (s, 4H, 2 x CH_2MOM), 4.72 (m, 1H, CH), 4.46 (m, 4H, 2 x CH_2), 3.61 (s, 6H, 2 x CH_3MOM), 3.50 (s, 12H, 4 x CH_3MOM), 2.23 (q, J = 7.56 Hz, 2H, CH_2), 1.13 (t, J = 7.43 Hz, 3H, CH_3).

*2.1.11. Bis-O-[3,4,5-tris(methoxymethoxy)galloy]-N-dodecanoyl serinol (**9**)*

Following the general procedure, **3** (50 mg, 0.18 mmol) was treated with **7** (Gazak et al., 2011) (120 mg, 0.40 mmol), HATU (152 mg, 0.40 mmol) and DMAP (244.34 mg, 0.44 mmol) to afford 72 mg (47 %) of the title compound as an amorphous white solid. ^{1}H-RMN (300 MHz, CD_3Cl) δ 7.57 (s, 4H, Ph), 6.01 (d, J = 8.30 Hz, 1H, NH), 5.24 (s, 8H, 4 x CH_2MOM), 5.22 (s, 4H, 2 x CH_2MOM), 4.73 (m, 1H, CH), 4.45 (m, 4H, 2 x CH_2), 3.61 (s, 6H, 2 x CH_3MOM), 3.51 (s, 12H, 4 x CH_3MOM), 2.18 (t, J = 7.28 Hz, 2H, CH_2), 1.59 (m, 2H, CH_2), 1.25 (m, 16H, 8 x CH_2), 0.87 (t, J = 6.92 Hz, 3H, CH_3).

*2.1.12. Bis-O-[3,4,5-tris(methoxymethoxy)galloy]-N-octadecanoyl serinol (**10**)*

Following the general procedure, **4** (50 mg, 0.14 mmol) was treated with (Gazak et al., 2011) (90.68 mg, 0.30 mmol), HATU (114 mg, 0.30 mmol) and DMAP (42.8 mg, 0.34 mmol) to afford 100.48 mg (75 %) of the title compound as an amorphous white solid. ^{1}H-RMN (300 MHz, CD_3Cl) δ 7.56 (s, 4H, Ph), 6.02 (d, J = 8.30 Hz, 1H, NH), 5.24 (s, 8H, 4 x CH_2MOM), 5.22 (s, 4H, 2 x CH_2MOM), 4.72 (m, 1H, CH), 4.44 (m, 4H, 2 x CH_2O), 3.60 (s, 6H, 2 x CH_3 MOM), 3.50 (s, 12H, 4 x CH_3 MOM), 2.05 (t, J = 7.2 Hz, 2H, CH_2CO), 1.44 (m, 2H, CH_2), 1.17 (m, 28H, 14 x CH_2), 0.81 (t, J = 6.92 Hz, 3H, CH_3).

Downloaded from jpet.aspetjournals.org at ASPET Journals on April 19, 2024

JPET Fast Forward. Published on June 5, 2018 as DOI: 10.1124/jpet.118.248278
This article has not been copyedited and formatted. The final version may differ from this version.

*2.1.13. Bis-O-[3,4,5-tris(methoxymethoxy)galloy]-N-oleoyl serinol (**11**)*

Following the general procedure, **5** (50 mg, 0.14 mmol) was treated with **7** (Gazak et al., 2011) (90.68 mg, 0.30 mmol), HATU (114 mg, 0.30 mmol) and DMAP (42.8 mg, 0.34 mmol) to afford 106 mg (81%) of the title compound as an amorphous white solid. ^{1}H-RMN (300 MHz, CD_3Cl) δ 7.52 (s, 4H, Ph), 6.02 (d, J = 8.20 Hz, 1H, NH), 5.33 (m, 2H, CH=CH), 5.24 (s, 8H, 4 x CH_2MOM), 5.22 (s, 4H, 2 x CH_2MOM), 4.73 (m, 1H, CH), 4.46 (m, 4H, 2 x CH_2), 3.61 (s, 6H, 2 x CH_3MOM), 3.51 (s, 12H, 4 x CH_3MOM), 2,19 (t, J = 8.55 Hz, 2H, CH_2), 1.99 (m, 2H, CH_2), 1.59 (m, 4H, 2 x CH_2), 1.27 (m, 20H, 10 x CH_2), 0.88 (t, J = 7.44 Hz, 3H, CH_3).

*2.1.14. Bis-O-[3,4,5-tris(methoxymethoxy)galloy]-N-linoleoyl serinol (**12**)*

Following the general procedure, **6** (50 mg, 0.14 mmol) was treated with **7** (Gazak et al., 2011) (90.68 mg, 0.30 mmol), HATU (114 mg, 0.30 mmol) and DMAP (42.8 mg, 0.34 mmol) to afford 98.72 mg (76%) of the title compound as an amorphous white solid. ^{1}H-RMN (300 MHz, CD_3Cl) δ 7.52 (s, 4H, Ph), 6.00 (d, J = 8.20 Hz, 1H, NH), 5.34 (m, 4H, 2 x CH=CH), 5.24 (s, 8H, 4 x CH_2MOM), 5.22 (s, 4H, 2 x CH_2MOM), 4.73 (m, 1H, CH), 4.46 (m, 4H, 2 x CH_2), 3.61 (s, 6H, 2 x CH_3MOM), 3.50 (s, 12H, 4 x CH_3MOM), 2.76 (t, J = 7.70 Hz, 2H, CH_2), 2.19 (m, 2H, CH_2), 2.03 (m, 4H, 2 x CH_2), 1.29 (m, 16H, 8 x CH_2), 0.88 (t, J = 8.01 Hz, 3H, CH_3).

*2.1.15. Synthesis of the deprotected serinol derivatives **13-17***

A solution of the corresponding MOM protected derivative in methanol was treated with aqueous hydrochloric acid (37%). The solution was stirred at room temperature overnight and then evaporated to dryness. The residue was co-evaporated several times with dichloromethane and then purified by triturating with cold diethyl ether. The precipitate that appeared was filtered and washed repeatedly with gently quantities of cold dichloromethane and diethyl ether to afford the corresponding unprotected derivative as a white solid.

*2.1.16. Bis-O-galloy]-N-propanoyl serinol (**13**)*

Following the general procedure, **8** (73 mg) was dissolved in methanol (1.5 mL) and treated with aqueous HCl 37% (0.08 mL) to give 41.4 mg (90%) of the title compound as a white amorphous solid. ^{1}H-

Downloaded from jpet.aspetjournals.org at ASPET Journals on April 19, 2024

JPET Fast Forward. Published on June 5, 2018 as DOI: 10.1124/jpet.118.248278
This article has not been copyedited and formatted. The final version may differ from this version.

RMN (400 MHz, DMSO-d_6) δ 8.08 (d, J = 8.10 Hz, NH), 6.96 (s, 4H, Ph), 4.39 (m, 1H, CH), 4.23 (m, 4H, 2 x CH_2O), 2.09 (q, J = 7.60 Hz, 2H, CH_2), 0.97 (t, J = 7.60 Hz, 3H, CH_3). ^{13}C-RMN (75 MHz, DMSO-d_6) δ 173.35, 165.75, 145.61, 138.66, 119.19, 108. 86, 62.98, 47.08, 38.31, 28.56, 10.01. MS (ES+): m/z 452.1 $(M+H)^+$ Anal. $C_{20}H_{21}NO_{11}$ (C, H, N, O).

*2.1.17. Bis-O-galloy]-N-dodecanoyl serinol (**14**)*

Following the general procedure, **9** (79 mg) was dissolved in methanol (1.5 mL) and treated with aqueous HCl 37% (0.08 mL) to give 51.3 mg (95%) of the title compound as a white amorphous solid. ^{1}H-RMN (400 MHz, DMSO-d_6) δ 9.25 (s, 6H, OH), 8.08 (d, J = 8.10 Hz, NH), 6.96 (s, 4H, Ph), 4.39 (m, 1H, CH), 4.23 (m, 4H, 2 x CH_2O), 2.09 (q, J = 7.60 Hz, 2H, CH_2), 1.50 (m, 2H, CH_2), 1,17 (m, 16H, 8 x CH_2), 0.97 (t, J = 7.60 Hz, 3H, CH_3). ^{13}C-RMN (75 MHz, DMSO-d_6) δ 165.05, 144.08, 137.99, 108.12, 62.33, 30.66, 28.39, 28.35, 28.24, 28.15, 28.09, 21.47, 13.33. MS (ES+): m/z 578.2 $(M+H)^+$. Anal. $C_{29}H_{39}NO_{11}$ (C, H, N, O).

*2.1.18. Bis-O-galloy]-N-octadecanoyl serinol (**15**)*

Following the general procedure, **10** (70 mg) was dissolved in methanol (1.5 mL) and treated with aqueous HCl 37% (0.08 mL) to give 39 mg (92%) of the title compound as a white amorphous solid. ^{1}H-RMN (400 MHz, DMSO-d_6) δ 9.13 (s, 6H, OH), 8.07 (d, J = 6.94 Hz, NH), 6.93 (s, 4H, Ph), 4.38 (m, 1H, CH), 4.21 (m, 4H, 2 x CH_2O), 2.05 (t, J = 7.20 Hz, 2H, CH_2CO), 1.43 (m, 2H, CH_2), 1.17 (m, 28H, 14 x CH_2), 0.81 (t, J = 7.08 Hz, 3H, CH_3). ^{13}C-RMN (75 MHz, DMSO-d_6) δ 172.5, 165.7, 145.5, 138.6, 119.1, 108.7, 63.0, 46.9, 38.3, 35.4, 31.3, 29.1, 28.9, 28.8, 28.7, 28.6, 25.3, 22.1, 14.0. MS (ES+): m/z 662.3 $(M+H)^+$. Anal. $C_{35}H_{51}NO_{11}$ (C, H, N, O).

*2.1.19. Bis-O-galloy]-N-oleoyl serinol (**16**)*

Following the general procedure, **11** (71.4 mg) was dissolved in methanol (1.5 mL) and treated with aqueous HCl 37% (0.08 mL) to give 45.9 mg (90%) of the title compound as a white amorphous solid. ^{1}H-RMN (400 MHz, DMSO-d_6) δ 9.23 (s, 4H, OH), 8.96 (s, 2H, OH), 8.07 (d, J = 6.94 Hz, NH), 6.95 (s, 4H, Ph), 5.28 (m, 2H, CH=CH), 4.40 (m, 1H, CH), 4.22 (m, 4H, 2 x CH_2), 2.06 (t, J = 7.20 Hz, 2H, CH_2), 1.92 (m, 4H, 2CH_2), 1.44 (m, 2H, CH_2), 1.20 (m, 20H, 10 x CH_2), 0.82 (t, J = 7.08 Hz, 3H, CH_3). ^{13}C-RMN (75

Downloaded from jpet.aspetjournals.org at ASPET Journals on April 19, 2024

MHz, DMSO-d_6) δ 172.4. 165.7, 145.5, 138.6, 129.7, 129.6, 119.1, 108.7, 63.0, 46.9, 35.4, 31.3, 29.1, 28.8, 28.7, 28.6, 28.5, 26.6, 25.3, 22.1, 14.0. MS (ES+): m/z 660.3 $(M+H)^+$. Anal. $C_{35}H_{49}NO_{11}$ (C, H, N, O).

*2.1.20. Bis-O-galloy]-N-linoleoyl serinol (**17**)*

Following the general procedure, **12** (61.5 mg) was dissolved in methanol (1.5 mL) and treated with HCl 37% (0.08 mL) to give 42.5 mg (97%) of the title compound as a white amorphous solid. ^{1}H-RMN (400 MHz, DMSO- d_6) δ 8.07 (d, J = 6.94 Hz, NH), 6.93 (s, 4H, Ph), 5.26 (m, 4H, 2 x CH=CH), 4.38 (m, 1H, CH), 4.20 (m, 4H, 2 x CH_2), 2.71 (m, 2H, CH_2), 2.05 (t, J = 7.20 Hz, 2H, CH_2), 1.90 (m, 2H, CH_2), 1.43 (m, 2H, CH_2), 1.19 (m, 18H, 9 x CH_2), 0.80 (t, J = 7.08 Hz, 3H, CH_3). ^{13}C-RMN (75 MHz, DMSO-d_6) δ 172.7, 165.8, 145.6, 138.7, 129.9, 129.8, 127.9, 127.8, 119.2, 108.9, 63.1, 47.1, 35.5, 31.0, 29.2, 28.8, 28.7, 28.6, 26.7, 25.5, 25.3, 22.1, 14.1. MS (ES+): m/z 658.3 $(M+H)^+$. Anal. $C_{35}H_{47}NO_{11}$ (C, H, N, O).

*2.1.21. Bis-O-[2,3-bis(benzyloxy)benzoyl]-N-oleoyl serinol (**19**)*

A solution of the Bn protected benzoic acid **18** (Belin et al, 2003) (166 mg, 0.49 mmol), HATU (214 mg, 0.56 mmol) and DMAP (41.5, 0.33 mmol) in dry CH_2Cl_2 (7.5 ml) was stirred at room temperature for 15 minutes and then added to a second solution, also stirred for 15 min, containing the *N*-oleoyl serinol derivate **5** (80 mg, 0.22 mmol) and DMAP (41.5, 0.33 mmol) in dry CH_2Cl_2 (7.5 ml). The mixture was stirred at room temperature overnight and then evaporated to dryness. The residue was dissolved in ethyl acetate (20 mL) and washed successively with saturated solutions of citric acid (3 x 20 mL), $NaHCO_3$ (3 x 20 mL) and NaCl (1 x 20 mL). The organic layer was dried over anhydrous Na_2SO_4, filtered, and concentrated under vacuum. The residue was then purified by flash column chromatography using hexane/EtOAc (10:1 to 1:1) as the eluent to afford 174 mg (77 %) of the title compound as a white amorphous solid. ^{1}H-RMN (400 MHz, $CDCl_3$) δ 7.42-7.06 (m, 26H), 5.77 (d, 1H, NH), 5.33 (m, 2H, CH=CH), 5.13 (m, 8H, 4 x CH_2), 4.56 (m, 1H, CH), 4.39 (m, 2H, CH_2), 4.28 (m, 2H, CH_2), 4.26 ^{13}C-RMN (75 MHz, $CDCl_3$) δ 173.1, 166.0, 152.8, 148.5, 137.4, 136.6, 130.1, 129.9, 128.7, 128.6, 128.5, 128.3, 128.2, 127.7, 126.3, 124.2, 123.1, 118.3, 75.8, 71.4, 63.7, 47.4, 36.5, 32.0, 29.9, 29.7, 29.5, 29.4, 29.3, 27.4, 25.6, 22.8, 14.3.

*2.1.22. Bis-O-(2,3-dihydroxybenzoyl)-N-octadecanoyl serinol (**20**)*

Downloaded from jpet.aspetjournals.org at ASPET Journals on April 19, 2024

JPET Fast Forward. Published on June 5, 2018 as DOI: 10.1124/jpet.118.248278
This article has not been copyedited and formatted. The final version may differ from this version.

A solution of **19** (150 mg, 0.152 mmol) in THF/MeOH (1:1) containing 30% wt% of Pd/C (10%) was hydrogenated at 30 ºC overnight under atmospheric pressure using a reaction balloon filled with hydrogen gas and a glass flask as the reaction vessel. The Pd/C was filtered through Whastman ® filter paper 42 and the solvent was removed under reduced pressure to give a crude product which was then purified by triturating with cold diethyl ether and dichloromethane to afford 84 mg (87 %) of the title compound as a white amorphous solid. ^{1}H-RMN (400 MHz, DMSO-d_6) δ 10.27 (s, 2H, OH), 9.38 (s, 2H, OH), 8.12 (d, J = 8.20 Hz, NH), 7.26 (dd, J = 8.10 Hz, 2H, J = 0.60 Hz, 2H, Ph), 7.00 (dd, J = 7.80 Hz, J = 0.60 Hz, 2H, Ph), 6.70 (t, J = 7.90 Hz, 2H, Ph), 4,54 (m, 1H, CH), 4.38 (m, 4H, 2 x CH_2), 2.06 (t, J = 7.20 Hz, 2H, CH_2), 1.43 (m, 2H, CH_2), 1.16 (m, 28H, 14 x CH_2), 0.82 (t, J = 6.60 Hz, 3H, CH_3). ^{13}C-RMN (75 MHz, DMSO-d6) δ 172.6, 169.2, 149.5, 146.1, 120.8, 119.9, 118.8, 112.9, 64.0, 46.4, 35.4, 31.3, 30.4, 29.1, 29.0, 28.9, 28.8, 28.7, 28.5, 25.3, 22.1, 14.0. MS (ES+): m/z 630.4 $(M+H)^+$. Anal. $C_{35}H_{51}NO_9$ (C, H, N, O).

*2.1.23. N,N-bis[3,4,5-tris(benzyloxy)benzoyloxyethyl]oleoylamide (**23**)*

A solution of the benzyl protected gallic acid **21 (**Rivero-Buceta et al., 2015b) (263 mg, 0.60 mmol), HATU (258 mg, 0.68 mmol) and DMAP (52.5 mg, 0.40 mmol) in dry CH_2Cl_2 (10 ml) was stirred at room temperature for 15 minutes and then added to a second solution, also stirred for 15 min, containing **22** (100 mg, 0.27 mmol) and DMAP (52.5 mg, 0.40 mmol) in dry CH_2Cl_2 (10 ml). The mixture was stirred at room temperature overnight and then evaporated to dryness. The residue was dissolved in ethyl acetate (20 mL) and washed successively with saturated solutions of citric acid (3 x 20 mL), $NaHCO_3$ (3 x 20 mL) and NaCl (1 x 20 mL). The organic layer was dried over anhydrous Na_2SO_4, filtered, and concentrated under vacuum. The residue was then purified by flash column chromatography using hexane/EtOAc (4:1 to 1:1) as the eluent to afford 216 mg (66%) of the title compound as an amorphous white solid. ^{1}H-RMN (400 MHz, $CDCl_3$) δ 7.27 (m, 34H, Ph), 5.24 (m, 2H, CH=CH), 5.01 (m, 12H, CH_2), 4.36 (m, 4H, CH_2), 4.36 (m, 4H, CH_2), 3.66 (m, 4H, CH_2), 2.29 (m, 2H, CH_2),1.90 (m, 4H, 2 x CH_2),1.50 (m, H, CH_2), 1.17 (m, 20H, 10 x CH_2), 0.80 (t, J = 6.60 Hz, 3H, CH_3). ^{13}C-RMN (75 MHz, $CDCl_3$) δ 173.3, 166.1, 165.9, 152.8, 152.7, 136.8, 136.6, 130.1, 129.9, 128.7, 128.6, 128.3, 128.2, 128.1, 127.7, 127.6, 125.0, 124.5, 109.2, 100.5, 75.3, 71.4, 71.3, 63.0, 62.6, 45.7, 33.4, 32.1, 29.9, 29.7, 29.6, 29.5, 29.4, 27.3, 25.5, 22.8, 14.3.

*2.1.24. N,N-bis(3,4,5-trihydroxybenzoyloxyethyl)octadecanoylamide (**24**)*

Downloaded from jpet.aspetjournals.org at ASPET Journals on April 19, 2024

JPET Fast Forward. Published on June 5, 2018 as DOI: 10.1124/jpet.118.248278
This article has not been copyedited and formatted. The final version may differ from this version.

A solution of **23** (200 mg, 0.164mmol) in THF/MeOH (1:1) containing 30% wt% of Pd/C (10%) was hydrogenated at 30 ºC overnight under atmospheric pressure using a reaction balloon filled with hydrogen gas and a glass flask as the reaction vessel. The Pd/C was filtered through Whastman ® filter paper 42 and the solvent was removed under reduced pressure to give the crude product which was then purified by triturating with cold diethyl ether and dichloromethane to afford 58 mg (53 %) of the title compound as a white amorphous solid. ^{1}H-RMN (300 MHz, DMSO-d_6) δ 9.14 (s, 3H, OH), 6.91 (s, 4H, Ph), 4.27 (m, 4H, 2 x CH_2), 3.66 (m, 4H, 2 x CH_2), 2.31 (t, J = 7.20 Hz, 2H, CH_2), 1.41 (m, 2H, CH_2), 1.29 (m, 28H, 14 x CH_2), 0.81 (t, J = 6.60 Hz, 3H, CH_3). ^{13}C-RMN (75 MHz, $CDCl_3$) δ 172.6, 165.8, 165.7, 145.6, 145.5, 138.7, 138.5, 119.2, 118.9, 108.6, 61.9, 61.7, 46.8, 44.3, 32.1, 31.3, 29.1, 29.0, 28.9, 28.7, 24.9, 22.1, 14.0. MS (ES+): m/z 676.4 $(M+H)^+$. Anal. $C_{36}H_{53}NO_{11}$ (C, H, N, O).

2.2. Biological methods

Stock solutions for each compound were prepared by dissolving the corresponding compound in dimethyl sulfoxide (DMSO) and were stored at -20ºC in dark.

2.2.1. Cell culture

SW-480 and SW-620 colorectal cancer cell lines and CCD18-Co colonic fibroblastic colon cell line were obtained from the American Type Culture Collection (ATCC) and were maintained under standard conditions of temperature (37°C), humidity (95%) and carbon dioxide (5%). SW-620 and SW-480 colon cancer cell lines were cultured in Dulbecco's Modified Eagle Medium (DMEM, Gibco-Invitrogen, Grand Island, NY, USA) supplemented with 10% Fetal Bovine Serum (Gibco-Invitrogen), 2mM glutamine (BioWhittaker, Lonza Group, Basel, Switzerland) and 1% antibiotics-antifungal (containing 10,000 units/mL of penicillin base, 10,000 µg/mL of streptomycin base and 25,000 ng/mL of amphotericin B; Gibco-Invitrogen). CCD18-Co human colon fibroblasts (ATCC, CRL-1459) were grown in Minimum Essential Medium (MEM) supplemented with 10% fetal bovine serum, 1% antibiotic/antimycotic, 2 mM GlutaMAX, 0,1 mM Non-essential amino acids (NEAA) (Invitrogen).

2.2.2. Cell Viability Assay

The anti-proliferative and cytotoxicity properties of the compounds in SW-620 human colon cancer cell line were measured by MTT assay. SW-620 cells were seeded in 24-well plates in exponential growth phase

Downloaded from jpet.aspetjournals.org at ASPET Journals on April 19, 2024

JPET Fast Forward. Published on June 5, 2018 as DOI: 10.1124/jpet.118.248278
This article has not been copyedited and formatted. The final version may differ from this version.

using a density of 25 x 10^3 cells per well. After 24 h, culture media were replaced with 500 µl of fresh culture media containing serial concentrations of each compound (dissolved in DMSO) and the number of viable cells was determined at time zero (control growth wells) using the MTT assay, as described below for treated cells. After 48 hours of treatment, treated cells were incubated during 3 h at 37ºC with 3-(4,5-dimethylthiazol-2-yl)-2,5-diphenyltetrazolium bromide (MTT) (50µL/well at 5 mg/mL in PBS) (Sigma-Aldrich, St. Louis, MO, USA). Over that time, MTT containing media were removed and the MTT reduced to purple formazan by living cells was solubilized by adding 200 µL of DMSO per well. After 1 h with mixing and dark, reduced formazan product, proportional to the number of viable cells, was measured at 560 nm using a scanning spectrophotometer microplate reader (Biochrom Asys UVM 340 Microplate Reader, ISOGEN, De Meern, The Netherlands). The parameters IC_{50} (µM) (concentration needed for 50% inhibition of cell proliferation), GI_{50} (µM) (concentration needed for 50% growth inhibition), TGI (µM) (concentration needed for total growth inhibition) and LC_{50} (µM) (concentration needed for 50% cell death) were calculated according to the NIH definitions using a logistic regression.

For all compounds, at least three independent experiments with three replicates per concentration were performed.

2.2.3. Extracellular flux analysis of the oxygen consumption rate (OCR) and extracellular acidification rate (ECAR)

Mitochondrial respiration and glycolytic function were analyzed with the XFe96 Cell Bionalyzer and Cell Mito Stress Test and XF Glycolysis Stress kits respectively (Seahorse Biosciences, XFe96). Prior to the assay, optimal cell density and oligomycin tritation were determined.

Glycolysis and oxidative phosphorylation are the two main energy-producing pathways in the cell. Most cells possess the ability to switch between these two pathways, thereby adapting to changes in their environment. Glucose in the cell is converted to pyruvate (referred to as glycolysis), and then converted to lactate in the cytoplasm, or CO_2 and water in the mitochondria. The conversion of glucose to pyruvate, and subsequently lactate, results in a net production and extrusion of protons into the extracellular medium. This, results in the acidification of the medium which is directly measured by XF6 analyzer and reported as the acidification rate (ECAR).

The assay scheme is as follows: First, cells are incubated in the glycolysis stress test medium without glucose or pyruvate and basal ECAR is monitored. The first injection is a saturating concentration of

Downloaded from jpet.aspetjournals.org at ASPET Journals on April 19, 2024

JPET Fast Forward. Published on June 5, 2018 as DOI: 10.1124/jpet.118.248278
This article has not been copyedited and formatted. The final version may differ from this version.

glucose (10 mM). The cells catabolize this glucose to pyruvate through the glycolytic pathway, producing ATP, NADH, water, and protons. The extrusion of protons into the surrounding medium leads to an increase in basal ECAR. The difference between ECAR before (basal situation) and after the addition of glucose is a measurement of the rate of glycolysis (glycolysis rate).

The second injection is oligomycin, which inhibits ATP synthase. Oligomycin inhibits mitochondrial ATP production, and shifts the energy production to glycolysis, with the subsequent increase in ECAR which is monitored as the cellular maximum glycolytic capacity. The difference between glycolytic capacity and glycolysis rate defines glycolytic reserve.

The final injection is 2-deoxy-glucose (2-DG), a glucose competitor, which inhibits glycolysis through competitive binding to hexokinase, the first enzyme in the glycolytic pathway. The resulting decrease in ECAR confirms that the ECAR produced and monitored in the assay is due to glycolysis.

For glycoStress assay, 20000 cells were plated in a XFe-96 well plate and kept overnight (o/n) in complete media. The next day, culture medium was changed to 0 mM glucose, 2 Mm glutamine in non-buffered media to starve the cells for 1h. Basal ECAR was monitored (1 to 3 measurements). Next, 10 mM glucose was injected to determine the capacity of the cells to upregulate glycolysis from the basal situation (4 to 6 measurements) and difference between basal ECAR and ECAR in the presence of glucose was determined to calculate Glycolysis value. Next, oligomycin was added to block ATP production from mitochondrial respiration to determine the maximal glycolytic capacity. Finally, 50 mM DG was injected to block completely glycolytic pathway.

The Cell Mito Stress Test measures key parameters of mitochondrial respiration by measuring the oxygen consumption rate (OCR) of cells. Cell Mito Stress Test uses sequential drug injections to target different electron transport chain (ETC) complexes in the mitochondria. In this way different parameters such as basal respiration, ATP production, proton leak, maximal respiration, spare respiratory capacity, and nonmitochondrial respiration were determined. Injections are as follow: oligomycin injection to inhibit ATP synthase (complex V), FCCP injection to uncouple oxygen consumption from ATP production, and rotenone and antimycin A injection to inhibit complexes I and III, respectively.

As indicated, oligomycin inhibits ATP synthase (complex V), and the decrease in OCR following injection of oligomycin correlates to the mitochondrial respiration associated with cellular ATP production.

Carbonyl cyanide-4 (trifluoromethoxy) phenylhydrazone (FCCP) is an uncoupling agent which disrupts the mitochondrial membrane potential and thus, electron flow through the electron transport chain (ETC)

Downloaded from jpet.aspetjournals.org at ASPET Journals on April 19, 2024

is inhibited, and oxygen is maximally consumed by complex IV. The FCCP-stimulated OCR is used to calculate spare respiratory capacity, defined as the difference between maximal respiration and basal respiration. Spare respiratory capacity is a measure of the ability of the cell to respond to increased energy demand.

The third injection is a mix of rotenone, a complex I inhibitor, and antimycin A, a complex III inhibitor. This combination shuts down mitochondrial respiration and enables the calculation of nonmitochondrial respiration driven by processes outside the mitochondria. Proton leak which is the remaining basal respiration not coupled to ATP production, can be a sign of mitochondrial damage or can be used as a mechanism to regulate the mitochondrial ATP production.

For mitostress assay, 40000 cells were plated and kept o/n in complete media. The next day, culture medium was changed to 10 mM glucose, 2 mM glutamine, 1 mM pyruvate non-buffered media and cells were kept for 1h at 37 ºC in an incubator without CO_2 Basal OCR was monitored (1 to 3 measurements). Next, 1µM oligomycin was injected to determine the amount of oxygen dedicated to ATP production at mitochondria (3 to 6 measurements). Then, carbonyl cyanide-4-(trifluoromethoxy)phenylhydrazone (FCCP) was injected at 0.4 µM to free H^+ gradient from the intermembrane space to the mitochondrial matrix, and so to determine the maximal respiration rate (MRR) or Spare Respiratory Capacity. Finally, antimycin A and rotenone (0.5µM) were added to completely inhibit mitochondrial respiration (7 to 9 measurements).

2.2.4. Western blot

Cells were lysed in Laemmli buffer, proteins were separated by SDS–polyacrylamide gel electrophoresis and transferred onto a nitrocellulose membrane (Bio-Rad Laboratories, Hercules, CA, USA). The membranes were blocked using 5% nonfat dry milk in TBS 0.05% Tween-20. Primary antibodies were incubated overnight at 4ºC and upon 1h incubation with secondary antibodies signal detection was performed using the Clarity Western ECL Substrate (Bio-Rad). β-actin determination or Ponceau stain were used as loading controls.

2.2.5. Caspase activation assay

SW-620 cells were plated in 96-multiwell and treated for 48 hours with 1.66 µM concentration of compounds **16** and **14**. Staurosporin (1.5 µM) was used as a positive control. Activity of caspase 3 and

Downloaded from jpet.aspetjournals.org at ASPET Journals on April 19, 2024

JPET Fast Forward. Published on June 5, 2018 as DOI: 10.1124/jpet.118.248278
This article has not been copyedited and formatted. The final version may differ from this version.

caspase 7 was quantified using the Caspase-Glo 3/7 assay kit (Promega), following manufacturer's instructions.

2.2.6. Measurement of cellular ATP content

Relative cellular ATP content was measured by the ATP based assay CellTiter-Glo Luminescent Cell Viability kit (Promega, Madison, WI, USA; Cat # G7571) with modifications from the manufacturer's protocol. Briefly, after 48h of treatment with compound **16** at IC_{50} (0.83 μM) and 2 x IC_{50} (1.66 μM), SW-620 cells were plated in 96-well clear bottom black polystyrene plates. 10000 cells were plated per well. Non-treated cells were plated in a similar way. Cells were then maintained for 6 h in complete media, without treatments, to allow cells to attach to the plate. Then, an equal volume of the single-one-step reagent provided by the kit was added to each well and rocked for 15 minutes at room temperature. Cellular ATP content was measured by a luminescent plate reader.

2.2.7. Statistical analysis

Dose-response curves for cell viability assays were analyzed by analysis of variance (ANOVA) with Bonferroni and Tukey as post hoc tests. Data were presented as mean ± SEM of at least three independent experiments each performed in triplicate. Statistical significance was defined as *$p<0.05$, **$p<0.01$; ***$p<0.001$. The statistical analyses were performed by use of the R statistical software version 2.15 (www.r-project.org).

Downloaded from jpet.aspetjournals.org at ASPET Journals on April 19, 2024

JPET Fast Forward. Published on June 5, 2018 as DOI: 10.1124/jpet.118.248278
This article has not been copyedited and formatted. The final version may differ from this version.

3. Results

3.1. Chemical results

For the synthesis of the proposed final compounds, the key *N*-acyl serinol derivatives (**2-6**) were prepared first (Scheme 1). Selective *N*-acylation of 2-amino-1,3-propanediol (serinol, **1**) was undertaken by reaction of the commercially available serinol with the corresponding acyl chlorides in the presence of triethylamine at -20 ºC to afford compounds **2-6** in good yields (70-81 %). It should be mentioned that the synthesis of these compounds were previously described in the literature following different procedures (Bieberich, 2002a; Bieberich, 2002b; Landau, 2014; Merg et al., 2015; Schulz and Robins, 2004; Oette and Tschung, 1980; Osornio et al., 2012). In our case, a unique procedure that implies the use of acyl chlorides and triethylamine has been followed for all of them.

Subsequently, condensation of the *N*-acyl serinol derivatives (**2-6**) with the MOM-protected galloyl acid (3,4,5-tris(methoxymethoxy)benzoic acid) (**7**) in the presence of HATU, as coupling reagent, and DMAP as base, followed by deprotection of the MOM ether intermediates **8-12** with aqueous hydrochloric acid (37%), gave the deprotected final compounds **13-17** in good yields (Scheme 2). It should be mentioned that the MOM-protected galloyl intermediate **7** was previously synthesized by other authors (Gazak et al., 2011). In our case, a modification of the previously described procedure, that implies the use of methyl gallate as starting material, gives this compound with good overall yield (60% for the two steps) (Scheme 2).

Next, compound **20**, with two 2,3-dihydroxybenzoyl residues, instead of galloyl, as phenolic substituents, was prepared (Scheme 3). In this case, the *N*-oleynol serinol derivative **5** was treated with the benzyl-protected benzoic acid **18** (Belin et al. 2003) in the presence of HATU, as coupling reagent, and DMAP as base (Scheme 3) to give **19** (77%). Catalytic hydrogenation of **19**, at atmospheric pressure in the presence of 10% Pd/C, afforded the fully deprotected derivative **20** in 87% yield (Scheme 3).

The same synthetic methodology was applied for the synthesis of compound **24**, in which diethanolamine, instead of serinol, has been used as linker (Scheme 4). In this case, the 3,4,5-benzyl protected galloyl **21** (Belin et al., 2003) was used as the phenolic synthon. Condensation of **21** with the corresponding *N*-oleoyl diethanolamine derivative **22** (Bieberich et al., 2002c; Sagnella et al., 2011) afforded **23** that was submitted to catalytic hydrogenation, using H_2/Pd-C, to give the deprotected derivative **24 (**53% yield).

Downloaded from jpet.aspetjournals.org at ASPET Journals on April 19, 2024

JPET Fast Forward. Published on June 5, 2018 as DOI: 10.1124/jpet.118.248278
This article has not been copyedited and formatted. The final version may differ from this version.

3.2. Inhibition of colon cancer cell growth

Firstly, the anti-proliferative properties of the new synthetic phenolic derivatives (**13-17, 20** and **24**) were tested in SW-620 human colon cancer cell line. Compound **SF6**, containing two galloyl moieties at both ends of a C12 *N*-acyl chain, from our collection of phenolic derivatives, was included for comparative purposes (Rivero-Buceta et al., 2015a) and 4,4´-Di-O-methylellagic acid, an effective phenolic compound against colon cancer cells (Ramirez de Molina et al., 2015) was used as the reference drug. The results are shown in Table 1.

Compound **SF-6** did not show any growth-inhibitory effect at the concentration tested (up to 100 μM) (Table 1) while compound **14**, in which the two galloyl units are at the same side of the C12 *N*-acyl chain affected human colon cell viability in the μM range. This data points to the importance for the growth-inhibitory effect of a polar "head", with two galloyl subunits.

Compound **13**, with one short *N*-acyl chain (C3) resulted inactive at the concentration tested. Further elongation of the length of the *N*-acyl chain led to an increase in the inhibitory activity. Thus, among the galloyl derivatives with a saturated *N*-acyl chain (**13-15**) the best inhibitory effect was observed for compound **15**, containing a C18 alkyl substituent, followed by **14**, containing a C12 alkyl chain.

On the other hand, the growth-inhibitory effect observed for compound **16**, with an unsaturated C18 chain, is better than that obtained for **15**, with a saturated C18 chain, and also better than that of **17**, with two double bonds in the acyl chain.

Compound **20** with a C-18 alkyl chain and where the phenolic substituents contain only 2 hydroxyl groups, was 22-fold less active than its corresponding C18 analogue (**15**), with two gallic acid residues (3 OHs on the aromatic ring).

On the basis of all of these results, it can be concluded that the cell growth inhibition depends significantly on both the size and unsaturation of the alkyl chain on the "tail" and the presence of galloyl groups on the "head".

The importance of serinol as the linker is supported by the loss of activity of the compound **24**, with an ethylene amine as linker, with respect to those observed for **15**, with serinol as linker. This result indicates that simple changes in structure can result in differences in growth inhibition, being serinol the best linker.

Finally, for comparative purposes we considered that it could be of interest to determine the growth-inhibitory effect of compound **16**, the most potent, in the cancer cell line SW480 (Table 2). SW480 and

Downloaded from jpet.aspetjournals.org at ASPET Journals on April 19, 2024

JPET Fast Forward. Published on June 5, 2018 as DOI: 10.1124/jpet.118.248278
This article has not been copyedited and formatted. The final version may differ from this version.

SW620 are colon carcinoma cell lines from a single patient derived either from the primary tumor (SW480) or from a lymph node metastasis (SW620) of the same tumor. SW620 cells are more highly tumorigenic and metastatic than SW480 (Hewitt et al., 2000).

As it was shown in Table 2 the human colon cancer cell line SW480 is also growth inhibited by **16**, although to different extent than SW620 cell line. In fact, a better inhibitory effect of **16** in SW620 cells than in SW480 cells (IC_{50} = 0.83 μM *vs* IC_{50} = 4.03 μM) was observed. This result can be of great therapeutic interest due to the fact that SW620 is much more aggressive than SW480.

Differences in sensitivity between those two cell lines towards a particular drug have also been described in the literature (R. Rashmi et al., 2003). Those differences might be explained by proteomic and metabolic differences between those cell lines that required further studies.

3.3. Toxicity in non-cancer cells

Next, toxicity in non-cancers cells for compound **16**, the one with the highest growth inhibitory effect, was determined. With this purpose, CCD18-Co colonic fibroblastic colon cell line was used. The IC_{50} for compound **16** in these primary epithelial colonic cells was 30 μM *vs* 0.83 μM in SW-620 colon cancer cells. This result indicates that there exists a therapeutic window for the use of compound **16** in colon cancer.

3.4. Cell bioenergetic analysis

Very recently a rapid and easy experimental methodology has been developed to analyze the energetic metabolism of a cell (glycolysis and oxidative phosphorylation) in real time (Pike Winer and Wu, 2014; TeSlaa and Teitell, 2014). When applied to the anticancer-field, this novel methodology facilitates a better understanding of the cancer cell metabolism and may be useful to discover agents that target specific metabolic pathways.

Glycolysis, conversion of glucose to lactate with the production of two molecules of ATP, is monitored through the measurement of the Extra-Cellular Acidification Rate (ECAR) at the surrounding media while oxidative phosphorylation through the measurement of the Oxygen Consumption Rate (OCR). High levels in basal ECAR may be indicative of reliance on glycolysis to support cell proliferation. The response to an input of glucose after starvation, -this is, the increase in ECAR compared to the basal situation-, determines the preferential use of the glycolytic pathway *vs* oxidative mitochondrial pathway. On the other hand,

Downloaded from jpet.aspetjournals.org at ASPET Journals on April 19, 2024

JPET Fast Forward. Published on June 5, 2018 as DOI: 10.1124/jpet.118.248278
This article has not been copyedited and formatted. The final version may differ from this version.

monitorization of OCR allows to determine the dependency of the oxidative metabolism by the cell. Thus, high basal OCR indicates a highly active oxidative metabolism.

Taking all of this into consideration we investigated the role of compound **16** (IC_{50}: 0.83 μM), the one with the highest growth inhibitory effect, on cell bioenergy as a possible cause of its anticancer activity. With this aim we monitored ECAR and OCR as readouts of glycolysis and mitochondrial respiration respectively using an extracellular flux bioanalyzer (Seahorse Biosciences XF96). Compound **14** (IC_{50}: 29.5 μM), with a moderate effect on cell viability, was also evaluated for comparative purposes.

We first tested the effect of compound **16** on the glycolytic activity using a glycostress standard assay (Fig. 2). SW-620 cancer cells were pretreated for 48 h with **16** at two concentrations (0.83 μM = IC_{50} and 1.66 μM = 2 x IC_{50}). Similarly, SW-620 cancer cells were pretreated with **14** at 0.83 μM and 16.66 μM (1 fold and 20 fold of the IC_{50} showed for compound **16**). Then cells were re-suspended and plated overnight. The next day, media was changed and cells were glucose starved for 1h. Basal ECAR was monitored (1 to 3 measurements). Next, 10 mM glucose was injected to determine the capacity of the cells to increase glycolysis from the basal situation (4 to 6 measurements). The difference between ECAR before (basal situation) and after the addition of glucose is a measurement of the glycolytic rate (glycolysis rate). As it can be observed in Fig. 2, compound **16** at a concentration of 1.66 μM significantly reduced glycolysis rate compared to control situation.

When oligomycin was added to inhibit mitochondrial ATP synthase and to block ATP production from mitochondrial respiration, SW-620 cells increased their glycolytic flux to maintain cell bioenergetic homeostasis. This increase in the glycolytic flux in response to a deficiency in mitochondrial ATP production is known as glycolytic capacity. As shown in Figure 2, the glycolytic capacity was significantly diminished in the presence of a 2 x IC_{50} dose of **16**. On the contrary, cells treated with **14** behaved similarly to control cells even at the highest concentration tested (16.66 μM), reinforcing the idea that compound **14** is less bioactive than **16.**

The difference between glycolytic capacity and glycolysis rate defines glycolytic reserve. This parameter was also significantly diminished at 2 x IC_{50} dose of **16.**

From these assays, it can be concluded that in the presence of **16**, glycolysis of SW620 cancer cells as energetic pathway is diminished (reduced glycolysis rate, glycolytic capacity and glycolytic reserve).

We next analyzed mitochondrial respiration by monitoring the oxygen consumption rate (OCR) using a mitostress standard assay (Figure 3). For this purpose, SW-620 cells were treated for 48h with compound

Downloaded from jpet.aspetjournals.org at ASPET Journals on April 19, 2024

JPET Fast Forward. Published on June 5, 2018 as DOI: 10.1124/jpet.118.248278
This article has not been copyedited and formatted. The final version may differ from this version.

16 at 0.83 μM = IC_{50} and 1.66 μM = 2 x IC_{50}, and with compound **14** at 0.83 μM and 16.66 μM. Non-treated cells were kept as controls.

Basal respiration, that is, the energetic demand of the cells under baseline conditions, was measured first. As shown in Fig.3A, cells treated with compound **16** at both concentrations displayed a reduced basal respiration compared to **14**-treated cells and control cells.

All other parameters of mitochondrial function -ATP production, spare respiratory capacity and proton leak - were determined following sequential injections of specific inhibitors: oligomycin (inhibitor of ATP synthase), carbonyl cyanide-4-(trifluoromethoxy)phenylhydrazone (FCCP), a disrupter of mitochondrial membrane potential, and rotenone/antimycin A (inhibitors of complex I and III of electron transport chain) (Pike Winer and Wu, 2014).

OCR before oligomycin injection *minus* OCR after oligomycin injection determines the portion of oxygen dedicated to ATP production by mitochondria. As shown in Fig. 3A this parameter is significantly reduced in **16** treated cells at 2 x IC_{50} concentration compared to **14** treated cells and control non treated cells.

Next, FCCP, which mimics an increased physiological energy demand, was injected to determine the maximal respiration rate (MRR) or spare respiratory capacity. This parameter determines the amount of extra ATP that can be produced by the cell in case of a sudden increase of energy demand as well as how closely the cell is breathing to its theoretical maximum. As it can be observed in Fig. 3A, after adding FCCP, cells treated with compound **16** at 2 x IC_{50} dose, displayed a significant reduction on the reserve respiratory capacity parameter compared to **14** treated cells and control non treated cells.

Finally, antimycin A and rotenone were added to completely inhibit mitochondrial respiration. The difference between OCR after oligomycin injection and OCR after rotenone and antimycin A injection was used to determine the proton leak function. This parameter determines the remaining basal respiration not devoted to ATP production and can be a sign of mitochondrial damage. As it can be observed in Fig. 3A, cells displayed a significant reduction on proton leak at all tested concentrations of **16** compared to compound **14** treated cells and control non-treated cells.

Next, we run a similar assay to compare mitochondrial respiration of **16** and **14** treated cells at 2 x IC_{50} dose of each compound, this is 1.66 μM for **16** and 60 μM for **14.** As it is shown in Fig. 3B, **14** at 60 μM diminished mitochondrial function in a similar way than **16** at 1.66 μM. These results indicate that **14** is

Downloaded from jpet.aspetjournals.org at ASPET Journals on April 19, 2024

JPET Fast Forward. Published on June 5, 2018 as DOI: 10.1124/jpet.118.248278
This article has not been copyedited and formatted. The final version may differ from this version.

indeed effective on targeting mitochondrial respiration, but it requires a higher concentration than **16** (60 μM for **14** *vs* 1.66 μM for **16**) in accordance to the previously determined IC_{50} value.

The discovery that compound **16** affects cell bioenergetics in colon cancer cells allow us to propose that its anticancer activity might be due, at least in part, to this property. It should be highlighted that, different to other scenarios where the energetic metabolism is rewired from glycolysis to mitochondrial respiration (Dai et al., 2015) or the other way around (Tesori et al., 2015), treatment with **16** diminishes both.

3.5. AMPK activation

As it was previously mentioned, 5'-AMP-activated kinase (AMPK) is an energy sensor that regulates energy metabolism. This is a heterotrimeric Ser/Thr kinase complex characterized by a catalytic α subunit and two regulatory subunits (β,γ) (Zadra et al., 2015). For the full activity of the kinase, a phosphorylation at the residue Thr172 in the catalytic loop is required. The active phosphorylated form of AMPK (P-AMPK) inhibits essentially all anabolic pathways that promote cell growth (Faubert et al., 2013). Thus, in cancer where the energy demands of the cell are elevated, AMPK activators may suppress tumor growth. The role of AMPK as a tumor suppressor is supported by the observation that patients on treatment with metformin, an activator of AMPK, have a lower cancer incidence (Evans et al., 2005; Vazquez-Martin et al., 2009).

Due to the critical role of AMPK in the regulation of energy and redox homeostasis, we wanted to check if compound **16** can contribute to its activation. As shown in Fig. 4A, treatment of colon cancer cells with compound **16,** even at the lowest concentration (0.83 μM), significantly increased the amount of the phosphorylated active form of AMPK (P-AMPK (Thr_{172})). Consequently, the ratio P-AMPK(Thr_{172})/total AMPK (figure 4B) is higher for **16** compared to control cells. Importantly, compound **14** was also able to activate AMPK but it required a higher concentration than **16** (29.5 μM for **14** *vs* 1.66 μM for **16** (Figs 4A and B). These results indicate that the two structurally related polyphenols **16** and **14**, are able to activate AMPK, but **16** was 18 times more potent than **14**.

As SW620 cells treated with **16** showed defective mitochondrial ATP production, together with decreased aerobic glycolysis, leading to AMPK activation, we analyzed the effect of this compound on the cellular ATP content. For this purpose, colorectal cancer SW620 cells were treated for 48 h with compound **16** at two concentrations (0.83 μM = IC_{50} and 1.66 μM = 2 x IC_{50}). Then, 10000 viable cells of non-treated and treated cells were re-plated. After 6 h in complete media, without treatments, the ATP content was measured by mean of the ATP based assay CellTiter-Glo Luminescent Cell Viability kit (Promega). As

Downloaded from jpet.aspetjournals.org at ASPET Journals on April 19, 2024

JPET Fast Forward. Published on June 5, 2018 as DOI: 10.1124/jpet.118.248278
This article has not been copyedited and formatted. The final version may differ from this version.

shown in Figure 4C the cellular ATP content was significantly reduced with respect to the control (non-treated cells) in the presence of the highest concentration of **16** (1.66 μM) *(p*<0.038). From this study we concluded that compound **16** diminishes cell bioenergetics leading to AMPK activation as a sensor of ATP depletion.

3.6. Induction of apoptosis

Finally, as compound **16** inhibited cell viability, diminishing cell bioenergetics and activating AMPK, we wanted to determine if it might induce apoptosis.

Apoptosis is a vital biological process of multicellular organisms by which damaged, mutant and aged cells are eliminated in a programmed way. As previously mentioned, a variety of natural polyphenols, like curcumin or resveratrol, induces apoptotic cell death in a variety of cancer models. This process is mediated by the activation of some specific proteases named caspases (Oliver and Vallette, 2005; Reed, 2000). Apoptosis, mediated by caspase activation may result in induction of death in cancerous cells and therefore represent a promising strategy to develop cancer chemotherapeutics.

There are more than 13 known caspases (procaspases or active cysteine caspases) that can be detected using various types of caspase activity assays (Bayascas et al., 2002; García-Calvo et al., 1999; Le et al., 2002; Mooney et al., 2002; Nicholson and Thornberry, 1997; Thornberry et al., 1997; Thornberry and Lazebnik, 1998). Among them, caspase-3 and -7 are especially important because they play a key role in the apoptotic pathway. In fact, their activation is being considered as a typical hallmark of apoptosis.

In the present study, we wanted to check if induction of apoptosis could be also implicated in the observed cell growth inhibition promoted by **16**. With this purpose the activity of caspase 3 and 7 was monitored using a luminescent assay. For this assay a time period of 48 h has been chosen because in a previous experiment carried out to determine the effect of the tested compounds on cell viability at different times (24 h, 48 h and 72 h) it was found that 24 h is a period of time too short to induce cellular lethality while 72 h is too long, ending with the cell death of most cells (data not shown).

Thus, SW-620 cells were treated for 48 h with compounds **14** and **16**, both at 1.66 μM (2 fold of the IC_{50} showed for compound **16**). Staurosporine (1.5 μM) treated cells were used as positive control of caspase 3/7 activation. Staurosporine is an alkaloid isolated from *Streptomyces staurosporeus* known to activate apoptosis in several cancer cells (Yadav et al., 2015).

Downloaded from jpet.aspetjournals.org at ASPET Journals on April 19, 2024

JPET Fast Forward. Published on June 5, 2018 as DOI: 10.1124/jpet.118.248278
This article has not been copyedited and formatted. The final version may differ from this version.

As it is shown in Figure 5, activity of caspase 3/7 after 48 h was significantly increased in SW-620 treated cells with compound **16** compared to control and **14.** Remarkably, higher effect on caspase 3/7 activation was also observed with **16** compared to the positive control, staurosporine.

Our results showed that compound **16** is able to stimulate significantly caspase activation in SW-620 cancer cells.

4. Discussion

Although metabolic alteration is one of the oldest mechanisms associated with cancer development, only recently its targeting became a promising anticancer strategy. In fact, altered metabolism is now considered an emerging hallmark of cancer and researches in the field hope to find drugs that may lead to a new class of anticancer drugs (Jang et al., 2013). However, this field is in a very preliminary stage and the effective number of compounds under investigation as potential modulators of cell metabolism is still very poor. For this reason, the identification of metabolically active agents can be of great interest for anticancer therapies.

In this report we provide evidence of the inhibitory effects on colon cancer growth and metabolism of a new family of synthetic polyphenols. These compounds have a hydrophilic "head", composed of two galloyl (3,4,5-trihydroxybenzoyl) units, and a hydrophobic "tail" linked through a serinol moiety. They were very efficiently obtained (high yields and easy purifications) in three steps by *N*-acylation of serinol followed by coupling with methoxy methyl (MOM) protected gallic acid and deprotection with aqueous hydrochloric acid.

On the basis of the Structure-Activity-Relationship (SAR) studies performed on this family it appears that the presence of the two galloyl moieties at the same side of the molecules is essential for inhibitory growth, and that the length of the *N*-acyl chain is also crucial for activity, being compounds with C12 and C18 chain length the best. A decrease of the acyl chain length, reduction of the number of OHs on the aromatic ring or substitution of serinol by ethanolamine as linker lowers or eliminates their anticancer properties. However, the introduction of a double bond on the hydrophobic tail increases the inhibitory growth properties. Compound **16**, with an unsaturated C18 chain, showed the highest anti-proliferative effect in SW-620 colon cancer cells.

Our results indicate that compound **16** reduces the energetic metabolism (glycolysis and mitochondrial respiration) in SW-620 colon cancer cells at the same time that activates AMPK and caspase 3 and 7

Downloaded from jpet.aspetjournals.org at ASPET Journals on April 19, 2024

JPET Fast Forward. Published on June 5, 2018 as DOI: 10.1124/jpet.118.248278
This article has not been copyedited and formatted. The final version may differ from this version.

activity. All of these findings lead us to suggest that, through AMPK activation, compound **16** might lead to alterations in colon cancer cell bioenergy compromising cancer cell viability. Importantly, these anti-proliferative and pro-apoptotic effects have been shown to be selective for cancer cells, indicating a therapeutic window for the use of this compound.

Of particular interest is the simultaneous inhibition of the two main energy-producing pathways (glycolysis and oxidative phosphorylation) showed by **16** in colon cancer cells. In this respect, it has been recently postulated that the pharmacological inhibition of several complementary metabolic pathways (antimetabolic cooperativity) can be better to eliminate cancer cells than the inhibition of a single one (Marchetti et al., 2015).

5. Conclusion

As recently emphasized by Jang and coworkers (Jang et al., 2013) cancer cell metabolism has become one of the most exciting and promising fields for the development of new anticancer agents. Targeting cancer metabolism opens an opportunity to develop broadly applicable drugs that can treat multiple cancer types and hence may lead to a new class of anticancer drugs.

We concluded that the novel molecules here described, and in particular **16**, the most potent within this series, show antiproliferative properties in two different colon carcinoma cell lines (SW480 and SW620), reduces the energetic metabolism (glycolysis and mitochondrial respiration) in SW-620 colon cancer cells at the same time that activates AMPK and caspase 3 and 7 activity. Based on that, **16** and its analogues could serve as hits to develop a new class of therapeutic agents that target tumor metabolism. Of particular interest is the simultaneous inhibition of the two main energy-producing pathways (glycolysis and oxidative phosphorylation) showed by **16** in colon cancer cells. Further research is needed to fully elucidate the possible mechanism(s) of action to suppress tumor growth. This is a non-trivial task because many different metabolic enzymes, oncogenic signalling pathways or/and regulatory network can be implied.

Downloaded from jpet.aspetjournals.org at ASPET Journals on April 19, 2024

JPET Fast Forward. Published on June 5, 2018 as DOI: 10.1124/jpet.118.248278
This article has not been copyedited and formatted. The final version may differ from this version.

6. Acknowledgments

We acknowledge MA Bonache for help with the processing of the Supporting Information.

Downloaded from jpet.aspetjournals.org at ASPET Journals on April 19, 2024

JPET Fast Forward. Published on June 5, 2018 as DOI: 10.1124/jpet.118.248278
This article has not been copyedited and formatted. The final version may differ from this version.

7. Authorship Contributions

Authors declare no potential conflict of interest. All co-author participated sufficiently in the work to take responsibility for the content and all co-authors approved the final version.

Participated in research design: San-Félix, Pérez-Pérez, Quintela, Gómez de Cedrón, Ramirez de Molina, Reglero

Conducted experiments: Madrona, Jiménez, Vargas, Gómez de Cedrón

Performed data analysis: San-Félix, Gómez de Cedrón

Wrote or contributed to the writing of the manuscript: San-Félix, Gómez de Cedrón

Downloaded from jpet.aspetjournals.org at ASPET Journals on April 19, 2024

JPET Fast Forward. Published on June 5, 2018 as DOI: 10.1124/jpet.118.248278
This article has not been copyedited and formatted. The final version may differ from this version.

8. Supplemental data

Copies of ^{1}H and ^{13}C NMR spectra are included.

Downloaded from jpet.aspetjournals.org at ASPET Journals on April 19, 2024

References

Arts IC and Hollman PC (2005) Polyphenols and disease risk in epidemiologic studies. *Am J Clin Nutr* **81** (1 Suppl): 317S-325S.

Bayascas JR, Yuste VJ, Benito E, Garcia-Fernández J and Comella JX (2002) Isolation of AmphiCASP-3/7, an ancestral caspase from amphioxus (Branchiostoma floridae). Evolutionary considerations for vertebrate caspases. *Cell. Death Differ.* **9**: 1078–89.

Belin FBP, Ruiz K, Lacombe JM and Pucci B (2003) Synthetic gallic acid derivatives as models for a comprehensive study of antioxidant activity. *Helv Chim Acta* **86**: 247-265.

Bieberich E, Hu B, Silva J, MacKinnon S, Yu RK, Fillmore H, Broaddus WC and Ottenbrite RM (2002a) Synthesis and characterization of novel ceramide analogs for induction of apoptosis in human cancer cells. *Cancer Lett* **181**(1): 55-64.

Bieberich E, Hu B, Silva J, Mackinnon S, Yu RK and Ottenbrite RM (2002b) Novel ceramide analogs are new anti-cancer drugs. *Polymer Preprints (American Chemical Society, Division of Polymer Chemistry)* **43** (2): 756-757.

Bieberich E, Ottenbrite RM, Yu RK, Fillmore H and Broaddus WC (2002c) Hydroxyalkyl amide analogs of ceramide. US 6410597B1.

Boyer JZ, Jandova J, Janda J, Vleugels FR, Elliott DA and Sligh JE (2012) Resveratrol-sensitized UVA induced apoptosis in human keratinocytes through mitochondrial oxidative stress and pore opening. *J Photochem Photobiol B* **113**: 42-50.

Cerella C, Radogna F, Dicato M and Diederich M (2013) Natural compounds as regulators of the cancer cell metabolism. *Int J Cell Biol* **2013**: Article ID 639401.

Dai W, Wang F, Lu J, Xia Y, He L, Chen K, Li J, Li S, Liu T, Zheng Y, Wang J, Lu W, Zhou Y, Yin Q, Abudumijiti H, Chen R, Zhang R, Zhou L, Zhou Z, Zhu R, Yang J, Wang C, Zhang H, Zhou Y, Xu L and Guo C (2015) By reducing hexokinase 2, resveratrol induces apoptosis in HCC cells addicted to aerobic glycolysis and inhibits tumor growth in mice. *Oncotarget* **6**(15): 13703–13717.

Evans JM, Donnelly LA, Emslie-Smith AM, Alessi DR and Morris AD (2005) Metformin and reduced risk of cancer in diabetic patients. *BMJ* **330**: 1304-1305.

Faubert B, Boily G, Izreig S, Griss T, Samborska B, Dong Z and Jones RG (2013) AMPK is a negative regulator of the Warburg effect and suppresses tumor growth in vivo. *Cell Metab* **17**(1): 113-124.

Downloaded from jpet.aspetjournals.org at ASPET Journals on April 19, 2024

Flores A, Camarasa MJ, Pérez-Pérez MJ, San-Félix A, Balzarini J and Quesada E (2014) Multivalent agents containing 1-substituted 2,3,4-trihydroxyphenyl moieties as novel synthetic polyphenols directed against HIV-1. *Org Biomol Chem* **12**(28): 5278-5294.

Garcia-Calvo M, Peterson EP, Rasper DM, Vaillancourt JP, Zamboni R, Nicholson DW and Thornberry NA (1999) Purification and catalytic properties of human caspase family members. *Cell Death Differ*. **6**: 362–369.

Gazak R, Valentova K, Fuksova K, Marhol P, Kuzma M, Medina MA and Kren V (2011) Synthesis and antiangiogenic activity of new silybin galloyl esters. *J Med Chem* **54** (20): 7397-7407.

González-Vallinas M, González-Castejón M, Rodríguez-Casado A and Ramírez de Molina A (2013) Dietary phytochemicals in cancer prevention and therapy: a complementary approach with promising perspectives. *Nutr Rev* **71**(9): 585-599.

Hadi SM, Bhat SH, Azmi AS, Hanif S, Shamim U and Ullah MF (2007) Oxidative breakage of cellular DNA by plant polyphenols: a putative mechanism for anticancer properties. *Semin Cancer Biol* **17**(5): 370-376.

Hardie DG (2014) AMP-activated protein kinase: maintaining energy homeostasis at the cellular and whole-body levels. *Annu Rev Nutr* **34**:31-55.

Hewitt RE, McMarlin A, Kleiner D, Wersto R, Martin P, Tsoskas M, Stamp GWH, Stetler-Stevenson WG (2000) Validation of a model of colon cancer progression. *J. Pathol*. **192**: 446-454.

Hung CM, Su YH, Lin HY, Lin JN, Liu LC, Ho CT and Way TD (2012) Demethoxycurcumin modulates prostate cancer cell proliferation via AMPK-induced down-regulation of HSP70 and EGFR. *J Agric Food Chem* **60** (34): 8427-8434.

Jang M, Kim SS and Lee J (2013) Cancer cell metabolism: implications for therapeutic targets. *Exp Mol Med* **45**: e45.

Kim MY, Trude LJ and Wogan GN (2009) Apoptosis induced by capsaicin and resveratrol in colon carcinoma cells requires nitric oxide production and caspase activation. *Anticancer Res* **29** (10): 3733-3740.

Kubatka P, Kapinova A, Kello M, Kruzliak P, Kajo K, Vybohova D and Dobrota D (2016) Fruit peel polyphenols demonstrate substantial anti-tumour effects in the model of breast cancer. *Eur J Nutr* **55** (3): 955-965.

Downloaded from jpet.aspetjournals.org at ASPET Journals on April 19, 2024

Landau EM and Siegel JS (2014) Lipidic biomaterials for encapsulation and triggered release. *PCT Int. Appl.,* 2014056939.

Le DA, Wu Y, Huang Z, Matsushita K, Plesnila N, Augustinack JC, Hyman BT, Yuan J, Kuida K, Flavell RA and Moskowitz MA (2002) Caspase activation and neuroprotection in caspase-3-deficient mice after *in vivo* cerebral ischemia and *in vitro* oxygen glucose deprivation. *Proc. Natl. Acad. Sci. USA* 99, 15188–15193.

Li W, Saud SM, Young MR, Chen G and Hua B (2015) Targeting AMPK for cancer prevention and treatment. *Oncotarget* **6** (10): 7365-7378.

López-Lázaro M (2010) A new view of carcinogenesis and an alternative approach to cancer therapy. *Mol Med* **16** (3-4): 144-153.

Luo Z, Zang M and Guo W (2010) AMPK as a metabolic tumor suppressor: control of metabolism and cell growth. *Future Oncol* **6** (3): 457-470.

Marchetti P, Guerreschi P, Kluza J and Mortier L (2014) Metabolic features of melanoma: a gold mine of new therapeutic targets?. *Curr Cancer Drug Targets* **14** (4): 357-370.

Marchetti P, Guerreschi P, Mortier L and Kluza J (2015) Integration of Mitochondrial Targeting for Molecular Cancer Therapeutics. *Int J Cell Biol* **2015**: Article ID 283145.

Merg AD, Slocik J, Blaber MG, Schatz GC, Naik R and Rosi NL (2015) Adjusting the Metrics of 1-D Helical Gold Nanoparticle Superstructures Using Multivalent Peptide Conjugates. *Langmuir* **31**(34): 9492-9501.

Mooney LM, Al-Sakkaf KA, Brown BL and Dobson PR (2002) Apoptotic mechanisms in T47D and MCF-7 human breast cancer cells. *Br. J. Cancer* **87**: 909–917.

Nicholson DW and Thornberry NA (1997) Caspases: Killer proteases. *Trends Biochem. Sci.* **22**: 299–306.

Neuhouser ML (2004) Dietary flavonoids and cancer risk: evidence from human population studies. *Nutr Cancer* **50** (1): 1-7.

Oette K and Tschung TS (1980) On the biosynthesis of glyceride- and phosphoglyceride analogues from monoglyceride analogue 2-(linoleoylamino)-1,3-propanediol in rats (author's transl)]. *Hoppe Seylers Z Physiol Chem* **361** (8): 1179-1191.

Oliver L and Vallette FM (2005) The role of caspases in cell death and differentiation. *Drug Resist Updat* **8**(3): 163-170.

Downloaded from jpet.aspetjournals.org at ASPET Journals on April 19, 2024

Osornio YM, Uebelhart P, Bosshard S, Konrad F, Siegel JS and Landau EM (2012) Design and synthesis of lipids for the fabrication of functional lipidic cubic-phase biomaterials. *J Org Chem* **77**(23): 10583-10595.

Pelicano H, Martin DS, Xu RH and Huang P (2006) Glycolysis inhibition for anticancer treatment. *Oncogene* **25** (34): 4633-4646.

Pierini R, Gee JM, Belshaw NJ and Johnson IT (2008) Flavonoids and intestinal cancers. *Br J Nutr* **99 E Suppl 1**: ES53-59.

Pike Winer LS and Wu M (2014) Rapid analysis of glycolytic and oxidative substrate flux of cancer cells in a microplate. *PLoS One* **9 (**10**)**:e109916.

Ramírez de Molina A, Vargas T, Molina S, Sánchez J, Martínez-Romero J, González-Vallinas M, Martín-Hernández R, Sánchez-Martínez R, Gómez de Cedrón M, Dávalos A, Calani L, Del Rio D, González-Sarrías A, Espín JC, Tomás-Barberán FA and Reglero G. (2015) The ellagic acid derivative 4,4'-di-*O*-methylellagic acid efficiently inhibits colon cancer cell growth through a mechanism involving WNT16. *J Pharmacol Exp Ther* **353** (2): 433-444.

Rashmi R, Santhosh Kumar TR, Karunagaran D (2003) Human colon cancer cells differ in their sensitivity to curcumin-induced apoptosis and heat shock protects them by inhibiting the release of apoptosis-inducing factor and caspases. *FEBS Letters* **538**: 19-24.

Reed JC (2000) Mechanisms of apoptosis. *Am J Pathol* **157** (5): 1415-1430.

Rivero-Buceta E, Carrero P, Doyagüez EG, Madrona A, Quesada E, Camarasa MJ, Peréz-Pérez MJ, Leyssen P, Paeshuyse J, Balzarini J, Neyts J and San-Félix A (2015a) Linear and branched alkyl-esters and amides of gallic acid and other (mono-, di- and tri-) hydroxy benzoyl derivatives as promising anti-HCV inhibitors. *Eur J Med Chem* **92**: 656-671.

Rivero-Buceta E, Carrero P, Casanova E, Doyagüez EG, Madrona A, Quesada E, Peréz-Pérez MJ, Mateos R, Bravo L, Mathys L, Noppen, S, Kiselev E, Marchand C, Pommier Y, Liekens S, Balzarini J, Camarasa MJ and San-Félix A (2015b) Anti-HIV-1 activity of a tripodal receptor that recognizes mannose oligomers. *Eur J Med Chem* **106**: 132-143.

Sagnella SM, Conn CE, Krodkiewska I and Drummond CJ (2011) Nonionic diethanolamide amphiphiles with unsaturated C18 hydrocarbon chains: thermotropic and lyotropic liquid crystalline phase behavior. *Phys Chem Chem Phys* **13** (29): 13370-13381.

Downloaded from jpet.aspetjournals.org at ASPET Journals on April 19, 2024

Schulz TC and Robins AJ (2004) Neural differentiation of human embryonic stem cells using protease passaging techniques, and applications in treating neural disorders. *PCT Int Appl* 2004090096.

Shin SM, Cho IJ and Kim SG (2009) Resveratrol protects mitochondria against oxidative stress through AMP-activated protein kinase-mediated glycogen synthase kinase-3beta inhibition downstream of poly(ADP-ribose)polymerase-LKB1 pathway. *Mol Pharmacol* **76** (4): 884-895.

TeSlaa T and Teitell MA (2014) Techniques to monitor glycolysis. *Methods Enzymol* **542**: 91-114.

Tesori M, Piscaglia AC, Samengo D, Barba M, Bernardini C, Scatena R, Pontoglio A, Castellini L, Spelbrink JN, Maulucci G, Puglisi MA, Pani G and Gasbarrini A (2015) The multikinase inhibitor Sorafenib enhances glycolysis and synergizes with glycolysis blockade for cancer cell killing. *Sci Rep* **5:** 9149.

Teiten MH, Eifes S, Dicato M and Diederich M (2010) Curcumin-the paradigm of a multi-target natural compound with applications in cancer prevention and treatment. *Toxins* **2** (1): 128-162.

Thornberry NA, Rano TA, Peterson EP, Rasper DM, Timkey T, Garcia-Calvo M, Houtzager VM, Nordstrom PA, Roy S, Vaillancourt JP, Chapman KT and Nicholson DW (1997) A combinatorial approach defines specificities of members of the caspase family and granzyme B. Functional relationships established for key mediators of apoptosis. *J Biol Chem* **272**: 17907–17911.

Thornberry NA and Lazebnik Y (1998) Caspases: Enemies within. *Science* **281**: 1312–1316.

Vázquez-Martín A, Oliveras-Ferraros C, López-Bonet E and Menéndez JA (2009) AMPK: Evidence for an energy-sensing cytokinetic tumor suppressor. *Cell Cycle* **8** (22): 3679-3683.

Warburg O (1956) On the origin of cancer cells. *Science* **123** (3191): 309-314.

Yadav SS, Prasad CB, Prasad SB, Pand LK, Singh S, Pradhan S and Narayan G (2015) Anti-tumor activity of staurosporine in the tumor microenvironment of cervical cancer: An i*n vitro* study. *Life Sci* **133**: 21-28.

Zadra G, Batista JL and Loda M (2015) Dissecting the Dual Role of AMPK in Cancer: From Experimental to Human Studies. *Mol Cancer Res* **13** (7): 1059-1072.

Zhang Q, Cheng G, Qiu H, Zhu L, Ren Z, Zhao W, Zhang T and Liu L (2015) The p53-inducible gene 3 involved in flavonoid-induced cytotoxicity through the reactive oxygen species-mediated mitochondrial apoptotic pathway in human hepatoma cells. *Food Funct* **6** (5): 1518-1525.

Downloaded from jpet.aspetjournals.org at ASPET Journals on April 19, 2024

JPET Fast Forward. Published on June 5, 2018 as DOI: 10.1124/jpet.118.248278
This article has not been copyedited and formatted. The final version may differ from this version.

Footnotes

This work was supported by the Spanish Plan Nacional de Cooperación Público-Privada, Subprograma INNPACTO (IPT-2012-0213 060000, co-financed by the FEDER program); the Spanish MINECO [Project SAF2015-64629-C2-1-R (MINECO/FEDER)]; AGL2016-76736-C3-3-R (MINECO/FEDER); Regional government Comunidad de Madrid (P2013/ABI-2728, ALIBIRD-CM) and EU Structural Funds. The European Social Fund (Youth Employment Operational Program 2014-2020) finances a contract in practices to AJ.

AM and TV contributed equally to this work.

Downloaded from jpet.aspetjournals.org at ASPET Journals on April 19, 2024

JPET Fast Forward. Published on June 5, 2018 as DOI: 10.1124/jpet.118.248278
This article has not been copyedited and formatted. The final version may differ from this version.

LIST OF FIGURE LEGENDS

Fig 1. Target polyphenols with two "heads" and one "tail"

Table 1. Inhibitory effects of test compounds on SW-620 human colon cancer cell viability

Table 2. Sensitivity of SW-480 and SW-620 human colon cancer cells to compound **16**

Fig 2. Glycolytic activity in SW-620 colon cancer cells. Comparison of the glycolytic function in SW-620 non-treated cells *vs* **16** treated cells (0.83 μM and 1.66 μM) and **14** treated cells (0.83 μM and 16.66 μM). Glycolysis (difference from ECAR value in the presence of glucose and ECAR value in starved cells), Glycolytic Reserve (difference between ECAR after ATPase inhibition and ECAR after glucose injection), and Glycolytic Capacity (sum of Glycolysis rate and Glycolytic Reserve) are shown. Representative assay of two experiments. Each experiment contains 6 replicates per treatment.

Fig 3. Mitochondrial respiration in SW-620 colon cancer cells. (A) Mitochondrial respiration analysis by flux analysis of the OCR in SW-620 non-treated cells *vs* **16** treated cells (0.83μM and 1.66μM) and **14** treated cells (0.83 μM and 16.66 μM). **(B)** Mitochondrial respiration analysis by flux analysis of the OCR in SW-620 non-treated cells *vs* **16** treated cells (1.66 μM and 3.2 μM) and **14** treated cells (1.66 μM and 60 μM). Representative assays of two experiments. Each experiment contains 6 replicates per treatment.

Fig 4. Compound 16 leads to AMPK activation (A) Western blot analysis of P-(Thr_{172}) AMPK and total AMPK. SW-620 cells were treated for 48 h with compound **16** (d1: 0.83 μM; d2: 1.66 μM and d3: 2.5μM) and **14** (d1: 1.66 μM and d2: 29.5 μM) Representative experiment. (B) Western blot quantification of ratio P-(Thr_{172})AMPK/Total AMPK. (C) Measurement of the intracellular ATP content. Luminiscence units were registered for compound **16** treated cells (0.83 μM and 1.66 μM) and compared to control non-treated cells.

Fig 5. Caspase 3/7 activity. Activation of caspase 3 and 7 after 48 h treatment with compounds **14** (1.66 μM) and **16** (1.66 μM). SW-620 cells treated with Staurosporine (1.5 μM) was used as the positive control.

Downloaded from jpet.aspetjournals.org at ASPET Journals on April 19, 2024

JPET Fast Forward. Published on June 5, 2018 as DOI: 10.1124/jpet.118.248278
This article has not been copyedited and formatted. The final version may differ from this version.

Data represents means ± S.E.M of two independent experiments each performed in triplicate. Asterisks indicate statistical differences in treated cells with respect to the control (non-treated cells) *$p<0.05$, **$p<0.01$; ***$p<0.001$.

Scheme 1. Synthesis of the *N*-acyl serinol derivatives **(2-6)**. *Reagent and conditions*: (i) MeOH:THF (2:1), TEA, -20 ºC to room temperature (rt).

Scheme 2. Synthesis of **13-17**. *Reagent and conditions*: (i) a) MOMCl, b) HOLi/H_2O (ii) HATU, DMAP (iii) aqueous HCl (37%)

Scheme 3. Synthesis of **20**. *Reagent and conditions*: (i) HATU, DMAP (ii) H_2, Pd/C

Scheme 4. Synthesis of **24**. *Reagent and conditions*: (i) HATU, DMAP (ii) H_2, Pd/C

Downloaded from jpet.aspetjournals.org at ASPET Journals on April 19, 2024

JPET Fast Forward. Published on June 5, 2018 as DOI: 10.1124/jpet.118.248278
This article has not been copyedited and formatted. The final version may differ from this version.

Table 1. Inhibitory effects of test compounds on SW-620 human colon cancer cell viability

Compound	IC_{50} (μM)[a]	GI_{50} (μM)[b]	TGI (μM)[c]	LC_{50} (μM)[d]
13	>100	>100	>100	>100
14	29.5 ± 10.18	10.5 ± 1.55	56.25 ± 7.46	75.5 ± 5.42
15	2 ± 0	1.58 ± 0.08	10.33 ± 1.45	19.33 ± 2.85
16	0.83 ± 0.083	0.57 ± 0.067	14.47 ± 12.77	75 ± 25
17	2.67 ± 0.67	1.83 ± 0.083	>100	>100
20	43.33 ± 4.41	24.33 ± 8.29	>100	>100
24	5.17 ± 1.17	2.33 ± 0.33	36.67 ± 4.41	63.33 ± 8.33
SF-6	>100	>100	>100	>100
4,4'-Di-*O*-MEA[e]	5.97 ± 1.09	1.58 ± 0.18	143.3 ± 23.66	>100

Data are the mean ± SEM of at least three independent experiments each performed in triplicate.
[a] Effective concentration, or compound concentration required for 50% inhibition of cell proliferation, after 48h treatment.
[b] Compound concentration required for 50% cell growth inhibition, after 48h treatment.
[c] Compound concentration required for total cell growth inhibition, after 48h treatment.
[d] Compound concentration required for 50% cell death, after 48h treatment.
Data (>100); not significant activity found at 150 μM concentration, after 48h treatment.
[e] 4,4'-Di-*O*-MEA; 4,4'-Di-*O*-methylellagic acid.

Downloaded from jpet.aspetjournals.org at ASPET Journals on April 19, 2024

JPET Fast Forward. Published on June 5, 2018 as DOI: 10.1124/jpet.118.248278
This article has not been copyedited and formatted. The final version may differ from this version.

Table 2. Sensitivity of SW-480 and SW-620 human colon cancer cells to compound **16**

Colorectal cancer cell line	IC_{50} (µM)[a]	GI_{50} (µM)[b]	TGI (µM)[c]	LC_{50} (µM)[d]
SW-480	4.03 ± 0.183	2.67 ± 0.27	24.31 ± 15.32	84 ±17
SW-620	0.83 ± 0.083	0.57 ± 0.067	14.47 ± 12.77	75 ± 25

Data are the mean ± SEM of at least three independent experiments each performed in triplicate.
[a] Effective concentration, or compound concentration required for 50% inhibition of cell proliferation, after 48h treatment.
[b] Compound concentration required for 50% cell growth inhibition, after 48h treatment.
[c] Compound concentration required for total cell growth inhibition, after 48h treatment.
[d] Compound concentration required for 50% cell death, after 48h treatment.

Downloaded from jpet.aspetjournals.org at ASPET Journals on April 19, 2024

JPET Fast Forward. Published on June 5, 2018 as DOI: 10.1124/jpet.118.248278
This article has not been copyedited and formatted. The final version may differ from this version.

FIGURES AND SCHEMES

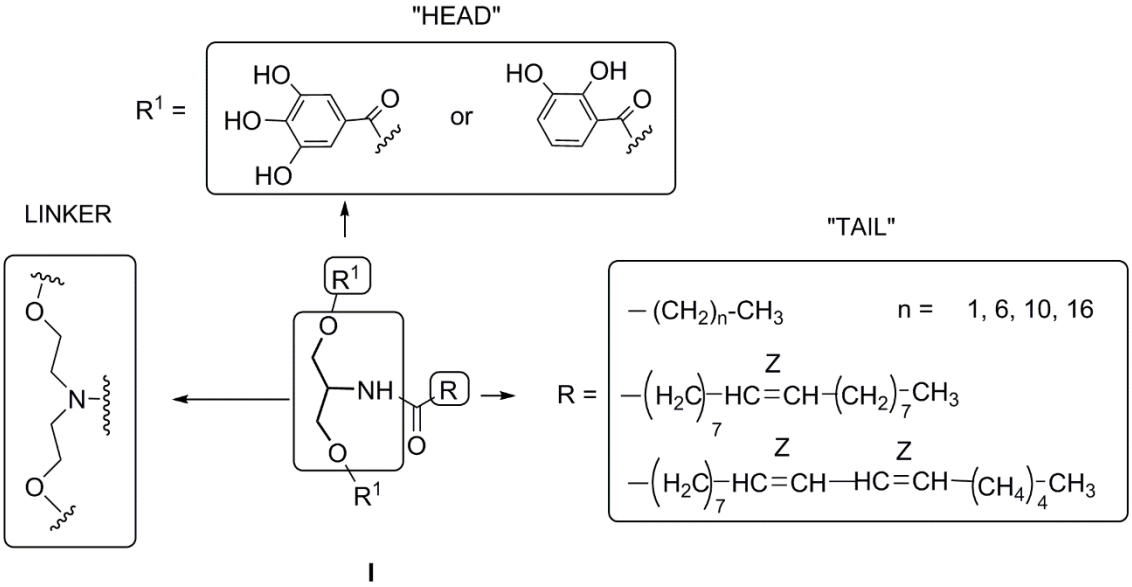

Fig 1. Target polyphenols with two "heads" and one "tail"

Downloaded from jpet.aspetjournals.org at ASPET Journals on April 19, 2024

JPET Fast Forward. Published on June 5, 2018 as DOI: 10.1124/jpet.118.248278
This article has not been copyedited and formatted. The final version may differ from this version.

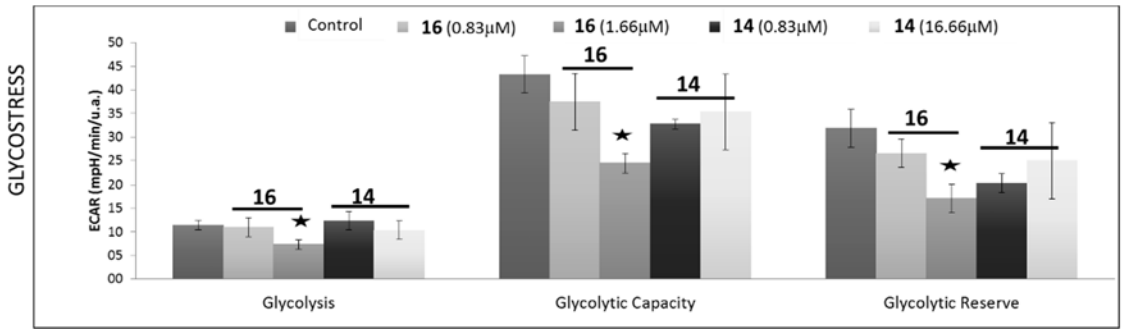

Fig 2. Glycolytic activity in SW-620 colon cancer cells. Comparison of the glycolytic function in SW-620 non-treated cells *vs* **16** treated cells (0.83 μM and 1.66 μM) and **14** treated cells (0.83 μM and 16.66 μM). Glycolysis (difference from ECAR value in the presence of glucose and ECAR value in starved cells), Glycolytic Reserve (difference between ECAR after ATPase inhibition and ECAR after glucose injection), and Glycolytic Capacity (sum of Glycolysis and Glycolytic Reserve) are shown. Representative assay of two experiments. Each experiment contains 6 replicates per treatment.

Downloaded from jpet.aspetjournals.org at ASPET Journals on April 19, 2024

JPET Fast Forward. Published on June 5, 2018 as DOI: 10.1124/jpet.118.248278
This article has not been copyedited and formatted. The final version may differ from this version.

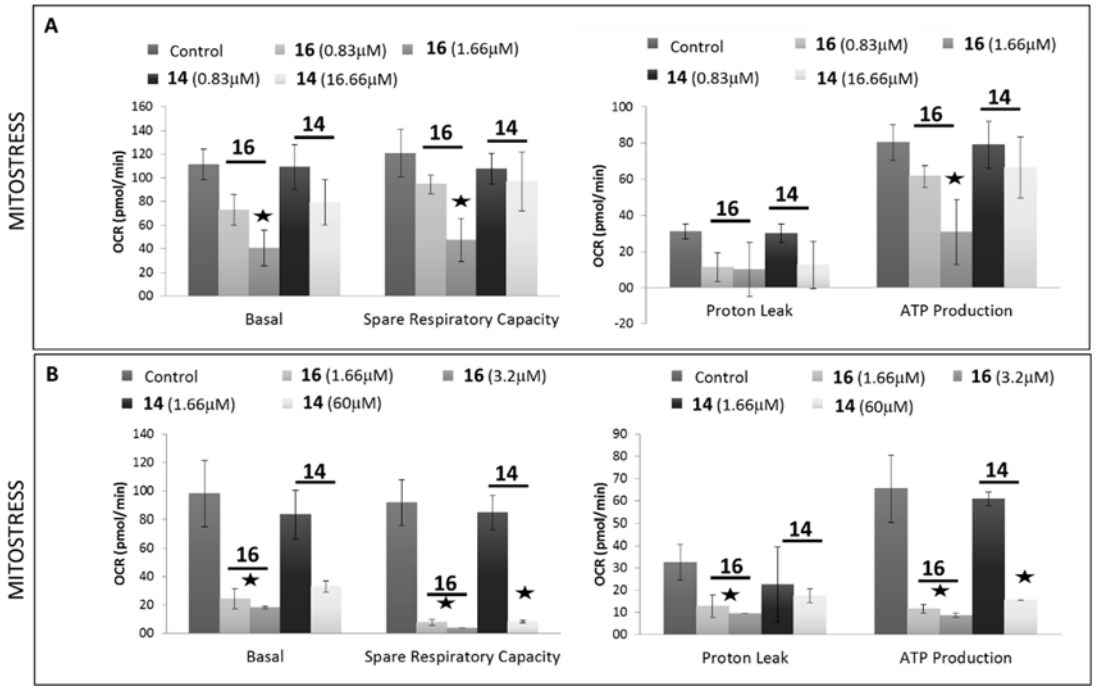

Fig 3. Mitochondrial respiration in SW-620 colon cancer cells. (A) Mitochondrial respiration analysis by flux analysis of the OCR in SW-620 non-treated cells *vs* **16** treated cells (0.83µM and 1.66µM) and **14** treated cells (0.83 µM and 16.66 µM). **(B)** Mitochondrial respiration analysis by flux analysis of the OCR in SW-620 non-treated cells *vs* **16** treated cells (1.66 µM and 3.2 µM) and **14** treated cells (1.66 µM and 60 µM). Representative assays of two experiments. Each experiment contains 6 replicates per treatment.

Downloaded from jpet.aspetjournals.org at ASPET Journals on April 19, 2024

JPET Fast Forward. Published on June 5, 2018 as DOI: 10.1124/jpet.118.248278
This article has not been copyedited and formatted. The final version may differ from this version.

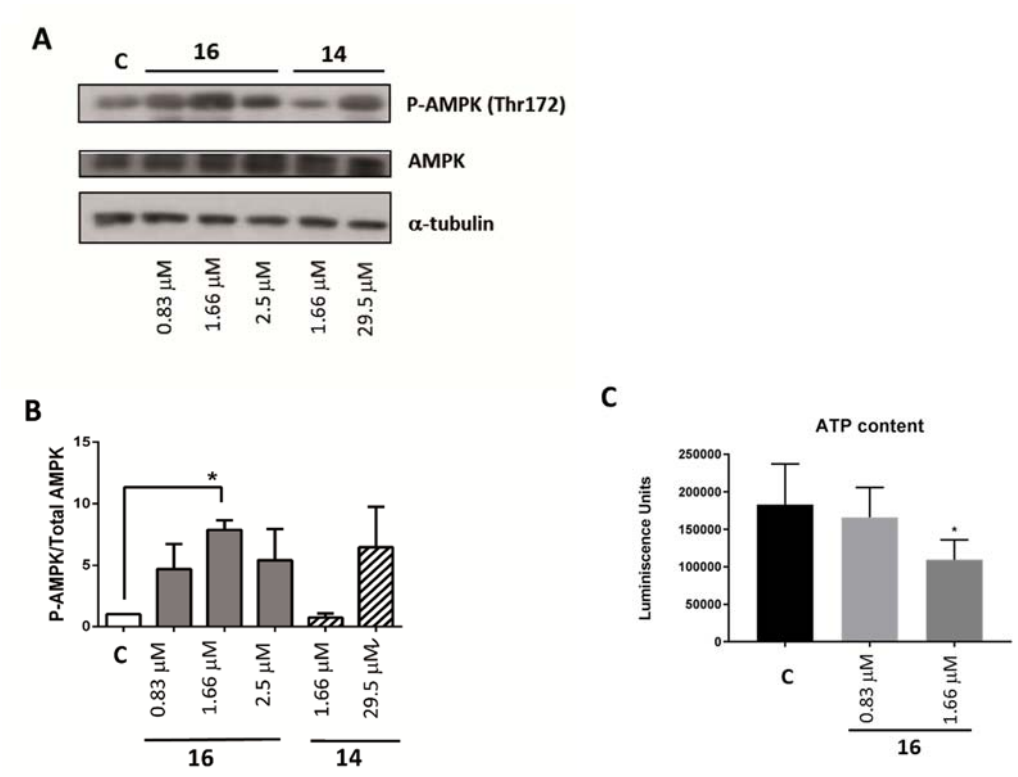

Fig 4. Compound 16 leads to AMPK activation (A) Western blot analysis of P-(Thr_{172})AMPK and total AMPK. SW-620 cells were treated for 48 h with compound **16** (d1: 0.83 µM; d2: 1.66 µM and d3: 2.5µM) and **14** (d1: 1.66 µM and d2: 29.5 µM) Representative experiment. (B) Western blot quantification of ratio P-(Thr_{172})AMPK/Total AMPK. (C) Effect of compound **16** on the cellular ATP content. SW620 cells were treated for 48 h with compound **16** at two different concentrations (0.83 µM = IC_{50} and 1.66 µM = 2 x IC_{50}), C = control (non-treated cells) (p<0.038).

Downloaded from jpet.aspetjournals.org at ASPET Journals on April 19, 2024

JPET Fast Forward. Published on June 5, 2018 as DOI: 10.1124/jpet.118.248278
This article has not been copyedited and formatted. The final version may differ from this version.

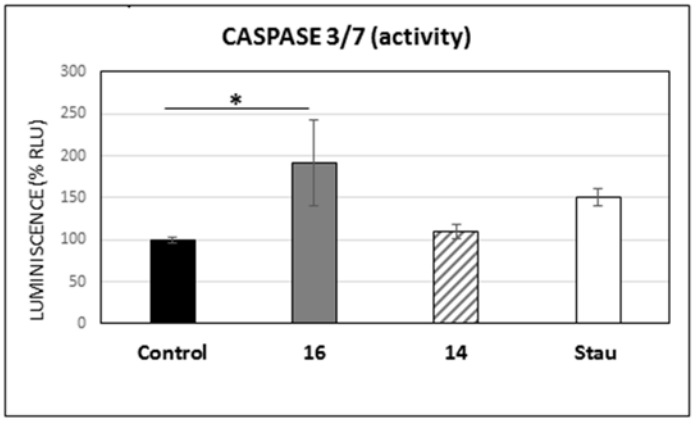

Fig 5. Caspase 3/7 activity. Activation of caspase 3 and 7 after 48 h treatment with compounds **14** (1.66 μM) and **16** (1.66 μM). SW-620 cells treated with staurosporine (1.5 μM) was used as the positive control. Data represents means ± S.E.M of two independent experiments each performed in triplicate. Asterisks indicate statistical differences in treated cells with respect to the control (non-treated cells) *$p<0.05$, **$p<0.01$; ***$p<0.001$.

Downloaded from jpet.aspetjournals.org at ASPET Journals on April 19, 2024

JPET Fast Forward. Published on June 5, 2018 as DOI: 10.1124/jpet.118.248278
This article has not been copyedited and formatted. The final version may differ from this version.

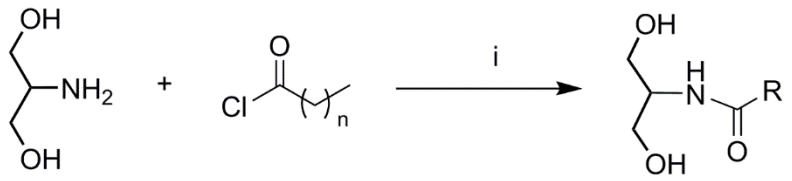

1

2, R = CH_2CH_3, 81%
3, R = $(CH_2)_{10}CH_3$, 80%
4, R = $(CH_2)_{16}CH_3$, 75%
5, R = $(CH_2)_7HC{=}CH(CH_2)_7CH_3$, 70%
6, R = $(CH_2)_7HC{=}CHCH_2HC{=}CH(CH_2)_4CH_3$, 79%

Scheme 1. Synthesis of the *N*-acyl serinol derivatives **(2-6)**. *Reagent and conditions*: (i) MeOH:THF (2:1), TEA, -20 ºC to room temperature (rt).

Downloaded from jpet.aspetjournals.org at ASPET Journals on April 19, 2024

JPET Fast Forward. Published on June 5, 2018 as DOI: 10.1124/jpet.118.248278
This article has not been copyedited and formatted. The final version may differ from this version.

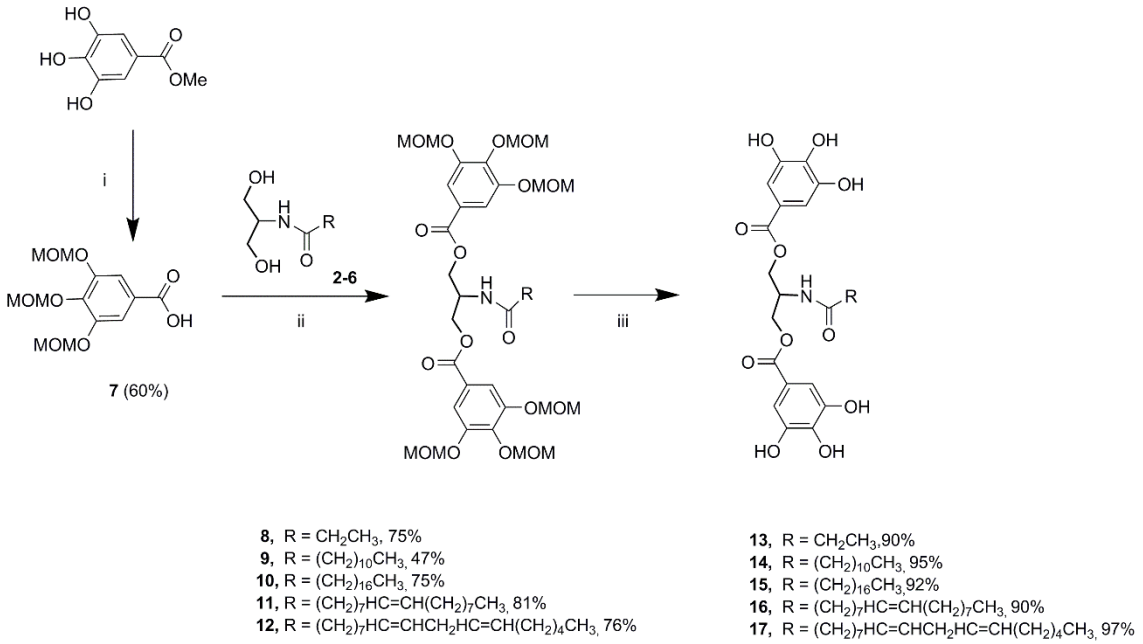

Scheme 2. Synthesis of **13-17**. *Reagent and conditions*: (i) a) MOMCl, b) HOLi/H_2O (ii) HATU, DMAP (iii) HCl

Downloaded from jpet.aspetjournals.org at ASPET Journals on April 19, 2024

JPET Fast Forward. Published on June 5, 2018 as DOI: 10.1124/jpet.118.248278
This article has not been copyedited and formatted. The final version may differ from this version.

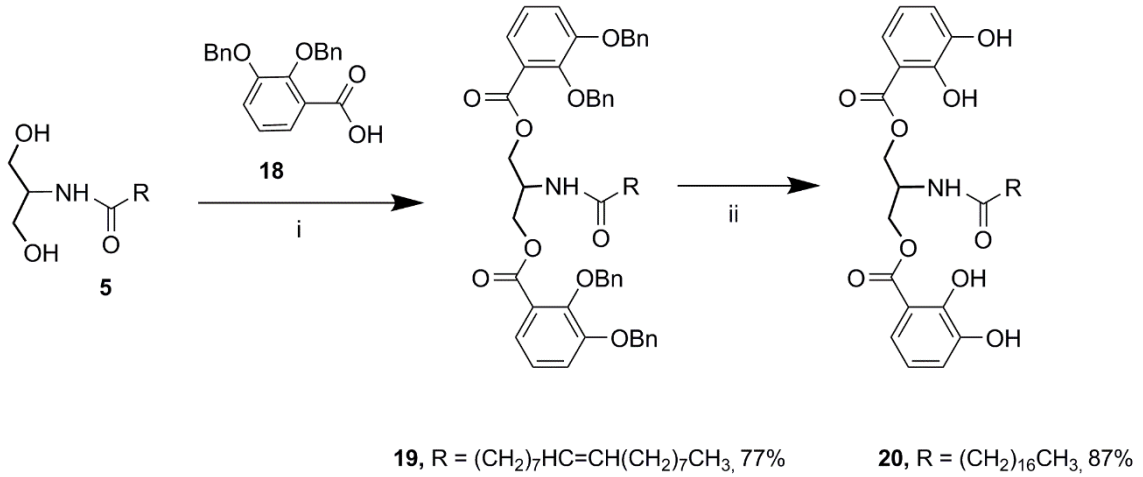

19, R = $(CH_2)_7HC{=}CH(CH_2)_7CH_3$, 77% **20,** R = $(CH_2)_{16}CH_3$, 87%

Scheme 3. Synthesis of **20**. *Reagent and conditions*: (i) HATU, DMAP (ii) H_2, Pd/C

Downloaded from jpet.aspetjournals.org at ASPET Journals on April 19, 2024

JPET Fast Forward. Published on June 5, 2018 as DOI: 10.1124/jpet.118.248278
This article has not been copyedited and formatted. The final version may differ from this version.

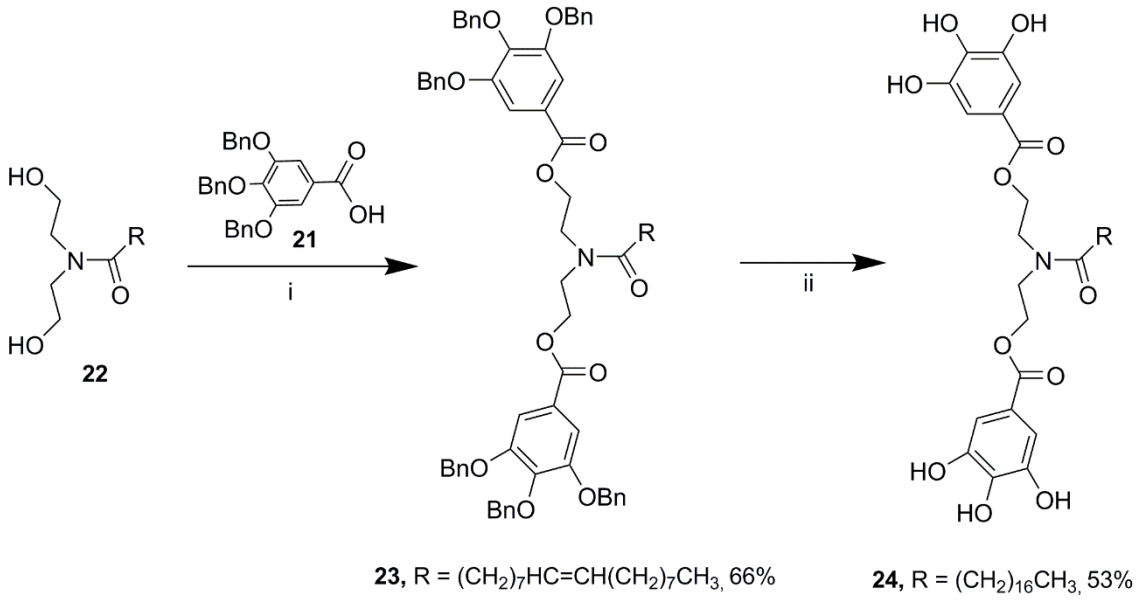

Scheme 4. Synthesis of **24**. *Reagent and conditions*: (i) HATU, DMAP (ii) H_2, Pd/C

Downloaded from jpet.aspetjournals.org at ASPET Journals on April 19, 2024